AD-A143 362 SPECIAL FINITE ELEMENTS FOR ANALYSIS OF SOIL CONSOLIDATION(U) OHIO STATE UNIV RESEARCH FOUNDATION COLUMBUS R S SANDHU ET AL. AUG 83 OSURF-715107-83-2 1/1

UNCLASSIFIED AFOSR-TR-84-0580 AFOSR-83-0055 F/G 8/13 NL

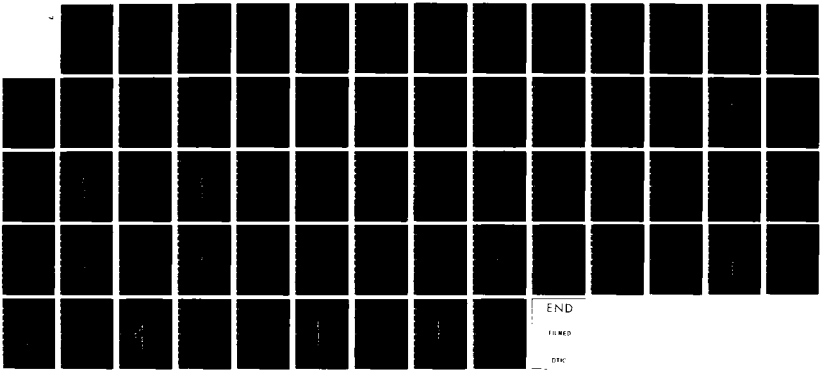

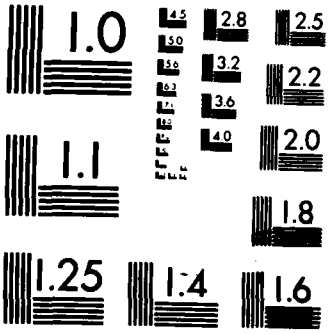

RF Project 763420/715107

SPECIAL FINITE ELEMENTS FOR ANALYSIS OF SOIL CONSOLIDATION

Ranbir S. Sandhu, Shyan Chyun Lee, and Hwie-Ing The
Department of Civil Engineering

DEPARTMENT OF THE AIR FORCE
Air Force Office of Scientific Research
Bolling Air Force Base, D.C. 20332

Grant No. AFOSR-83-0055

August, 1983

OSU
The Ohio State University
Research Foundation
1314 Kinnear Road
Columbus, Ohio 43212

UNCL

SECURITY CLASSIFI[illegible]IS PAGE

REPORT DOCUMENTATION PAGE

1a. REPORT SECURITY CLASSIFICATION UNCLASSIFIED	1b. RESTRICTIVE MARKINGS
2a. SECURITY CLASSIFICATION AUTHORITY	3. DISTRIBUTION/AVAILABILITY OF REPORT APPROVED FOR PUBLIC RELEASE; DISTRIBUTION UNLIMITED
2b. DECLASSIFICATION/DOWNGRADING SCHEDULE	
4. PERFORMING ORGANIZATION REPORT NUMBER(S)	5. MONITORING ORGANIZATION REPORT NUMBER(S) AFOSR-TR- 84-0580
6a. NAME OF PERFORMING ORGANIZATION The Ohio State University 6b. OFFICE SYMBOL (If applicable) NA	7a. NAME OF MONITORING ORGANIZATION AFOSR/NA
6c. ADDRESS (City, State and ZIP Code) 1314 Kinnear Road Columbus, Ohio 43212	7b. ADDRESS (City, State and ZIP Code) Building 410 Bolling AFB, DC 20332
8a. NAME OF FUNDING/SPONSORING ORGANIZATION AFOSR 8b. OFFICE SYMBOL (If applicable) NA	9. PROCUREMENT INSTRUMENT IDENTIFICATION NUMBER AFOSR-83-0055
8c. ADDRESS (City, State and ZIP Code) Building 410 Bolling AFB, DC 20332	10. SOURCE OF FUNDING NOS. PROGRAM ELEMENT NO.: 61102F PROJECT NO.: 2307 TASK NO.: C1 WORK UNIT NO.:
11. TITLE (Include Security Classification) Special Finite Elements for Analysis of Soil Consolidation	
12. PERSONAL AUTHOR(S)	
13a. TYPE OF REPORT Annual 13b. TIME COVERED FROM _____ TO _____	14. DATE OF REPORT (Yr., Mo., Day) August 1983 15. PAGE COUNT 62
16. SUPPLEMENTARY NOTATION	
17. COSATI CODES FIELD / GROUP / SUB. GR.	18. SUBJECT TERMS (Continue on reverse if necessary and identify by block number)

19. ABSTRACT (Continue on reverse if necessary and identify by block number)

Use of 'singularity' elements to model pore-pressures in the vicinity of free-draining loaded surfaces, immediately after application of loads at these surfaces is discussed. One-dimensional consolidation is considered. Comparison of numerical results with the exact solution shows that use of specially designed elements approaching 'singularity' may succeed in reducing the error in pore-pressures.

20. DISTRIBUTION/AVAILABILITY OF ABSTRACT UNCLASSIFIED/UNLIMITED ☒ SAME AS RPT. ☒ DTIC USERS ☐	21. ABSTRACT SECURITY CLASSIFICATION UNCLASSIFIED
22a. NAME OF RESPONSIBLE INDIVIDUAL LTC Lawrence D. Hokanson	22b. TELEPHONE NUMBER (Include Area Code) (202) 767-4935 22c. OFFICE SYMBOL AFOSR/NA

DD FORM 1473, 83 APR EDITION OF 1 JAN 73 IS OBSOLETE.

UNCLASSIFIED
SECURITY CLASSIFICATION OF THIS PAGE

OSURF-715107-83-2

SPECIAL FINITE ELEMENTS

FOR

ANALYSIS OF SOIL CONSOLIDATION

By

Ranbir S. Sandhu
Shyan Chyun Lee
Hwie-Ing The

August 1983

Prepared for:

AIR FORCE OFFICE OF SCIENTIFIC RESEARCH
Grant: AFOSR-83-0033

Geotechnical Engineering Report No. 9

THE OHIO STATE UNIVERSITY RESEARCH FOUNDATION

1314 Kinnear Road, Columbus, Ohio 43212

ABSTRACT

Use of 'singularity' elements to model pore-pressures in the vicinity of free-draining loaded surfaces, immediately after application of loads at these surfaces is discussed. One-dimensional consolidation is considered. Comparison of numerical results with the exact solution shows that use of specially designed elements approaching 'singularity' may succeed in reducing the error in pore-pressures.

TABLE OF CONTENTS

LIST OF FIGURES

LIST OF FIGURES(CONTINUED)

LIST OF TABLES

I. INTRODUCTION

Use of the finite element method for solution of soil consolidation problems is well established. Since the first application of this method [1,2], considerable progress has been made in the theoretical formulation as well as the computational procedures. Recent advances include variational formulations admitting limited smoothness of finite element bases [3,4], experimentation with several different spatial interpolation schemes [5-9] and investigation of various temporal approximation methods [6,9-15]. The finite element method has been applied to soils exhibiting secondary compression [8,11,13], nonlinear soil behavior [13,16-20], and to finite deformation [16,18,20]. Developments in solution procedures include use of Laplace transforms [10,11,14], automatic selection of the time-step size [13] and the use of single variable formulations [21,22]. Other developments cover use of boundary element methods [23,24], allowance for infinitely distant boundaries, material interfaces, etc.

One particular aspect of the finite element procedures for soil consolidation has been the difficulty in reproducing accurately the pore-water pressures near loaded free-draining surfaces immediately after application of loads at these surfaces. This can be troublesome in problems involving inelastic soil behavior. Yokoo's [25] formulation, not requiring the fluid pressure to satisfy the prescribed boundary condition at the free-draining boundary gave good solution immediately after loading. Buchmaier's [26] studies showed that transition elements, using higher order interpolation, near loaded boundaries had only limited success. Vermeer [27] suggested that the fluid pressure boundary condition be enforced as a 'ramp' condition to limit the error.

Herein we report numerical performance of another approach to development of finite element procedures to satisfactorily model the pore-pressure distribution in the vicinity of free-draining loaded surfaces. It consists of using 'singularity' elements. In the second section we state the two-field formulation of the boundary value problem of consolidation of linear elastic soils. The third section contains a discussion of the problem of determining the pore pressures in the vicinity of a free-draining loaded surface and a description of 'singularity' elements. The numerical performance of several variants of the scheme in solution of one-dimensional consolidation is discussed in the fourth section. The fifth section lists the conclusions arrived at as a result of this investigation.

II. EQUATIONS GOVERNING LINEAR ELASTIC SOIL CONSOLIDATION

II.A The Differential Equations

Assuming pore water to be incompressible, the equations of force equilibrium of elementary volumes and of mass continuity may be written in standard indicial notation as [1,7,28]:

$$[E_{klij}\, u_{k,l}]_{,i} + \Pi_{,j} + \rho f_j = 0 \tag{1}$$

$$[K_{ij}\,(\Pi_{,j} + \rho_2 f_{2i})]_{,i} + u_{i,i} = 0 \tag{2}$$

where $u_i, f_i, E_{klij}, K_{ji}$ denote the cartesian components, respectively, of the displacement vector, the body force vector per unit mass, the isothermal elasticity tensor and the permeability tensor. ρ is the mass density of the saturated soil and ρ_2 that of water. Π is the pore water pressure. With these field equations we associate the following boundary conditions:

$$u_i = \hat{u}_i \quad \text{on } S_{1i} \tag{3}$$

$$t_i = (\sigma_{ji} + \Pi\delta_{ji})n_j = \hat{t}_i \quad \text{on } S_{2i} \tag{4}$$

$$\Pi = \hat{\Pi} \quad \text{on } S_3 \tag{5}$$

$$Q = q_i n_i = \hat{Q} \quad \text{on } S_4 \tag{6}$$

where S_{1i}, S_{2i} are complementary subsets of the boundary of the spatial region of interest and so are S_3, S_4.

Discretization of the governing function for the two-field formulation [3,29] followed by application of the variational principle leads to the following matrix equations [1,29,30]:

$$\begin{bmatrix} K & C \\ C^T & \alpha\Delta t\bar{K} \end{bmatrix} \begin{Bmatrix} u(t_1) \\ \Pi(t_1) \end{Bmatrix} + \begin{bmatrix} 0 & 0 \\ C^T & -(1-\alpha)\Delta t K \end{bmatrix} \begin{Bmatrix} u(t_0) \\ \Pi(t_0) \end{Bmatrix} = \begin{Bmatrix} P_1 \\ P_2 \end{Bmatrix} \tag{7}$$

where (t_0, t_1) is the single time step of interest;

$$\Delta t = t_1 - t_0$$

$\{u(t_1)\}$, $\{u(t_0)\}$ = vectors of nodal point values of the components of displacement at time t_1, t_0 respectively;

$\{\pi(t_1)\}$, $\{\pi(t_0)\}$ = vectors of nodal point values of the pore water pressure at times t_1, t_0 respectively;

$\{P_1\}$ = the vector of nodal point loads including applied nodal loads, boundary tractions, body forces, initial stresses and effect of displacement constraints;

$\{P_2\}$ = the vector of nodal point fluxes including applied nodal fluxes, boundary fluxes, body force effects and effects of specified pore water pressures;

$[K]$ = the spatial 'stiffness matrix' for the elastic soil;

$[\bar{K}]$ = the spatial 'flow matrix' for $\alpha\Delta t = 1$;

α = the coefficient characterizing single step temporal discretization; $\alpha \geq .5$ for stabili

$[C]$ = the coupling matrix representing the influence of pore water pressures in the force equilibrium equation;

$[C]^T$ = the coupling matrix representing the influence of soil volume change upon the nodal point flux.

The matrices $[K]$ and $[\bar{K}]$ depend upon the interpolation schemes for displacements and pore water pressures, respectively. The coupling matrix $[C]$ involves spatial interpolation for both the field variables. The temporal discretization for the single step scheme is reflected in the value of the coefficient .

Equation (7) includes the 'natural' boundary conditions expressed by Equations (4) and (6). Equations (3) and (5) are satisfied by explicitly requiring $u_i = \hat{u}_i$ on S_{1i} and $\pi = \hat{\pi}$ on S_3.

II.8 Spatial Interpolation

The basic interpolation scheme used in the present study was the 8-4 quadrilateral element introduced by Sandhu [7,30]. In this element, the displacements have biquadratic lagrange interpolation and the pore water pressure has bilinear lagrange interpolation which is isoparametric with the element geometry. In this report, this procedure is referred to as the standard PS84 procedure. The singularity elements used near the loaded free-draining surfaces will be described in the next section.

III. PORE-PRESSURES NEAR LOADED FREE-DRAINING BOUNDARIES

III.A Preliminaries

Immediately after application of a surface load to a free-draining boundary, the excess pore water pressure remains zero at the surface but has a very steep gradient and rises, over an extremely short distance into the soil mass, to a magnitude comparable with the applied stress. Finite element interpolations commonly used do not have [29] the capability to model this locally high pore pressure gradient near the surface. Attempts to overcome this difficulty have included use of variational principles where the pressure field is not required to satisfy the specified boundary condition [25], using fine mesh near the loaded surface, and using higher order interpolation near the loaded surface [26]. None of these gives satisfactory results. During consolidation of nonlinear soils, the stress solution at any time step defines the mechanical behavior for the next step. Therefoe, it is important to get sufficiently accurate element stresses at each time step. In the work reported herein, an alternative approach based on use of special 'singularity elements' was used.

III.B Singularity Elements

Singularity elements, using special interpolation schemes which reflect the actual variation in the variables, have been extensively used for analysis of fracture where the stresses are unbounded at the crack-tip. Hughes and Akin [31] proposed special functions for point as well as line singularities. In the present work only line singularity was considered in the context of a two -dimensional problem.

Consider the sequence of functions

$$f_n(x) = 1 - x^n \tag{8}$$

over the domain [0,1]. Figure 1 shows the plots for n=0 through 5. In the limit as $n \longrightarrow \infty$, $f_n(x) = 1$ for x in the interval [0,1) and =0 at x=1. This is the type of discontinuity encountered in consolidation analysis. Two types of singularity elements were considered.

III.B.i The two-node singularity element

In one dimension, over range [0,1], the singularity element would use interpolation functions

$$1-x^n \ , \ x^n$$

where n is sufficiently large. For n=1 this reduces to linear interpolation. Noting that the error in pore water pressures near loaded free-draining boundaries is of relevance only immediately after loading and decays with advance in the time domain, it appeared reasonable to use a composite element which would approximate the singularity for small values of the 'elapsed time' after loading and reduce to linear interpolation for large

values of the time variable. This led to use of variants of the type

$$f_n(x) = 1 - ax - (1 - a)x^n \tag{9}$$

where a=0 approximates the singularity element and a=1 gives linear interpolation. Thus, the coefficient a has to be assigned a value growing with time from 0 to 1. The scheme investigated was based on

$$a = 1 - \exp(-a\tau) \tag{10}$$

where a is a scalar coefficient and τ the non-dimensional 'time factor'. The investigation covered a range of values of n and a.

III.B.ii The three-node singularity element

This element would directly involve three functions, viz.,

$$1,\ x,\ x^n$$

where n is sufficiently large. This was expected to include linear interpolation and approximation of the singularity at the same time.

III.B.iii Interpolation functions for the quadrilateral singularity elements

Special 8-4 and 8-6 elements were used to model the singularity. Figure 2 shows the arrangement for the two elements. The line singularity implies singularity in one variable only. In the following we assume this to be the variable t. For the 8-4 element the interpolating functions are:

$$\{N\} = \begin{Bmatrix} (1-s)(1-t^n) \\ s(1-t^n) \\ s\,t^n \\ (1-s)t^n \end{Bmatrix} \tag{11}$$

where the range of s, t is [0,1]. If the variant expressed by Equation (9) is employed;

$$\{N\} = \begin{Bmatrix} (1-s)(1-at-(1-a)t^n) \\ s(1-at-(1-a)t^n) \\ s(at+(1-a)t^n) \\ (1-s)(at+(1-a)t^n) \end{Bmatrix} \tag{12}$$

For the 8-6 element, the interpolating functions are:

$$\{N\} = \begin{Bmatrix} (1-s)((1-t^n)-(2-b)M) \\ s((1-t^n)-(2-b)M) \\ s(t^n-bM) \\ (1-s)(t^n-bM) \\ 2sM \\ 2(1-s)M \end{Bmatrix} \tag{13}$$

where

$$b = 2^{1-n}$$

and

$$M = (t-t^n)/(1-2(.5)^n)$$

IV. NUMERICAL PERFORMANCE

IV.A Introduction

Several investigators [33 thru' 39] have used the finite element method to obtain approximate solutions to the problem of soil consolidation. Using different interpolation schemes all have generally reported success with whatever scheme they used. Comparative evaluations of different schemes are rare. Some comparisons of numerical performance were attempted by Sandhu [7,8]. In evaluating various procedures, Sandhu [29] proposed that the following criteria be used.

i. The interpolation scheme must conform with the assumptions regarding continuity and differentiability used in setting up the governing variational formulation.

ii. It should be possible to generate the 'undrained' solution i.e., the state of fluid pressures and displacements at time t=0+.

iii. For sufficiently small time steps, the scheme should be insensitive to the choice of the time step size.

The 8-4 element is known to satisfy all the three conditions [7,8,29] except that near drained loaded surfaces, the solution at t = 0+ has an error which decays with advance in the time domain [7]. If the solution immediately after loading was of no interest, the 8-4 interpolation scheme would be adequate. However, if accuracy of the solution at t=0+is important (e.g. in nonlinear or cyclic consolidation), modifications to the element interpolation scheme are necessary. Indeed this was the primary motivation for the present investigation.

IV.B The Example Problem

The procedures described were applied to Terzaghi's problem of one dimensional consolidation. For this problem, the theoretical solution is known and, therefore, precise comparisons were possible. The dimensions of the consolidating soil column and the soil properties were the same as in Sandhu's example [7]. Figure 3 shows the soil column. Figure 4 shows the finite element model. The time domain was partitioned as tabulated below:

1 step of $\Delta t = 0$ to get the 'undrained' solution

1 step of $\Delta t = 0.00001$ over [0.0,0.00001]

1 step of $\Delta t = 0.01$ over [0.00001,0.01001]

9 steps of $\Delta t = 0.01$ over [0.01001, 0.10001]

10 steps of $\Delta t = 0.1$ over [0.10001, 1.10001]

10 steps of $\Delta t = 1.0$ over [1.10001, 11.10001]

9 steps of $\Delta t = 10.0$ over [11.10001, 101.10001]

10 steps of $\Delta t = 100.0$ over [101.10001, 1101.10001]

8 steps of Δt =1000.0 over [1101.10001, 9101.10001]

IV.C Results of the Analysis

The example problem was solved using the special singularity elements described earlier. The solution in each case gave nodal point values of the pore pressures. The error in the solution was non-dimensionalized through division by the applied surface load.

Figure 5A and Tables IA,IB show the history of pore water pressure using the 8-4 element with functions of the type expressed by Equation (8) at depth .03H below the top free-draining boundary of the soil column of height H. Results show that the 'immediate' pore water pressure obtained by this method was more accurate than the that obtained using the PS84. However, the pore pressure dropped sharply after application of the load and accuracy in pore pressures was worse than that of PS84 in later time stages. Apparently, the error in pore pressure at later time stages was due to the absence of the linear term from the interpolation scheme. For time factor values upto .03 the error reduced with n increasing upto 5. For time factor values greater than .3 the error increased with increasing n.

Figure 5B and Table IC show the results at a point .06H below the loaded surface. Figure 5C and Table ID give the results at a depth of .09H. As would be expected, the error at these points is throughout smaller than at .03H. The pattern of dependence upon n and the value of the time factor is essentially .pn 23 the same.

To combine the ability of the singularity interpolation to give accurate 'immediate' pore pressures and the accuracy of the PS84 element for later time stages, it appeared reasonable to set up shape functions such that the element has the characteristics of the singularity element at early stages and these change to those of PS84 as time increases. For this reason, shape functions of the type expressed by Equation (9) were developed. Figures 6A thru' 6F and Tables 2A thru' 2C show the effect of variation in a for values of n equal to 5,10,15,30,40 and 48. Figures 6G, 6H and Tables 2D, 2E give additional information, for n equal to 48, for the locations .06H and .09H below the surface.

Figure 7 compares the results for various values of n paired with the optimal(out of the set tried) value of a in each case. The least error in initial pore pressures was realized for n=48, a=40. However, the error was seen to grow with time. The best overall accuracy was obtained for n=30, a=32.5. For this case, the maximum error was less than three percent. Figures 8A thru' 8D show the spatial variation of error in the calculated pore pressures for this choice of n,a.

Figures 9A thru' 9D and Tables 3A thru' 3D illustrate the results obtained using the 8-6 singularity element. Accuracy of the pore pressure at any location of the entire soil column except .03H and .015H below the loaded surface is good. At later time stages also the pore pressures compared well with the exact solution and did not differ much from the results of the PS84 element regardless of the value of n (so long as it was greater than 5) in the singularity element; n=10 gave the best results.

Exact evaluation of the element matrices requires the Gaussian quadrature to use a number of integration points equal to the index n (for n an integer). This can be quite expensive. The CPU time using 48 integration points for only one element was about 50 percent more than that for the PS84 system. To reduce computational costs, use of reduced integration order for the 8-4 element, using interpolants in Equation (8) was investigated. The error in pore pressures, using five point integration, increased with n upto 20. Beyond this value of n the error decreased. The best results were obtained for n equal to 62.5. The results are summarized in Figures 10A thru' 10C and Tables 4A thru' 4D.

V. CONCLUSIONS

Numerical performance of the several schemes that were investigated indicates the following:

i. The 8-4 singularity element using shape functions based $f(x) = 1-x^n$ gives good values for the 'immediate' pore pressures but at later time stages the results are in error. Accuracy in pore water pressures at all time stages was improved using reduced order of quadrature for sufficiently high value of n.

ii. The 8-6 'singularity' element using shape functions based on $f(x)=a+bx+cx^n$, yielded good values of the pore pressures at all time stages for most of the soil column. However, at locations close to the loaded surface, the error was quite large. This makes the scheme unsatisfactory.

iii. Accuracy in pore pressures at all time stages can be achieved using the 8-4 'singularity' element whose shape functions are based on $f(x) = 1 - ax - (1-a)x^n$, in which the coefficient $a = 1 - \exp(-\alpha \overline{c})$. This combines the best characteristics of the singularity element with those of the PS84 element.

The foregoing conclusions are based on study of a one-dimensional problem. It is important that the procedures be extended to problems of two and three dimensions (point singularities as well as surface singularities) before firm recommendations for routine use of certain elements can be made. More investigation is also needed in the selection of indices n and a used in the formulation. Further, realizing that the consolidation of soils is a decay process, use of more that one exponential terms in the time domain could possibly enhance accuracy. Use of reduced integration in conjunction with interpolation of the type $f(x) = 1 - ax - (1 - a)x^n$, if successful, would reduce the computational costs.

VI. ACKNOWLEDGEMENTS

This report is based on the second author's M.S. thesis presented to the Ohio State University. The Ohio State University Instruction and Research Computer Center provided the computational facilities. The Air Force Office of Scientific Research provided partial support under Grant AFOSR-83-0055 to the Ohio State University.

VII. REFERENCES

1. R.S. Sandhu, Fluid Flow in Saturated Porous Media, Ph.D. Thesis, University of California, Berkeley, California, 1968.
2. R.S. Sandhu, and E.L. Wilson, "Finite Element Analysis of Seepage in Elastic Media", Proceedings, Amer. Soc. Civ. Engrs., Vol. 95, Jour. Engrg. Mech. Div., 641-652, 1969.
3. R.S. Sandhu, Variational Principles for Soil Consolidation, Report OSURF-3570-2 to National Science Foundation, Dept. of Civil Engineering, The Ohio State University, Columbus, Ohio, 1975.
4. R.S. Sandhu, "Variational Principles for Finite Element Analysis of Soil Consolidation", in Numerical Methods in Geomechanics, ED. C.S. Desai, Amer. Soc. Civ. Engrs., 20-40,-1976.
5. J. Ghaboussi, and E.L. Wilson, "Flow of Compressible Fluid in Porous Elastic Solids", Int. Jour. Numer. Methods in Engrg., Vol. 5, 419-442, 1973.
6. I.M. Smith, "Transient Phenomena of Offshore Foundations", in Numerical Methods in Offshore Engineering, Eds. O.C. Zienkiewicz, R.W. Lewis, and K.C. Stagg, J. Wiley, 483-513, 1978.
7. R.S. Sandhu, H. Liu, and K.J. Singh, "Numerical Performance of Some Finite Element Schemes for Analysis of Seepage in Porous Elastic Media", Int. Jour. Numer. Anal. Methods in Geomechanics", Vol. 1, 177-194, 1977.
8. R.S. Sandhu, and H. Liu, "Analysis of Consolidation of Viscoelastic Soils", in Numerical Methods in Geomechanics, Ed. W.Wittke, Balkema, 1255-1263, 1979.
9. J.H. Prevost, "Consolidation of Anelastic Porous Media", Proceedings, Amer. Soc. Civ. Engrs., Vol. 107, Jour. Engrg. Mech. Div., 169-186, 1981.
10. J.R. Booker, "A Numerical Method of Solution of Biot's Consolidation Theory", Quar. Jour. Mech. and App. Math., Vol. 26, 445-470, 1973.
11. J.R. Booker, and J.C. Small, "Finite Element Analysis of Primary and Secondary Consolidation", Int. Jour. Solids Struct., Vol. 13, 137-149, 1977.
12. I.M. Smith, J.L. Siemieniuch, and I. Gladwell, "Evaluation of Norsett Methods for Integrating Differential Equations in Time", Int. Jour. Numer. Anal. Methods in Geomechanics, Vol. 1, 57-74, 1977.
13. K. Runesson, On Nonlinear Consolidation of Soft Clay, Publication 78:1, Dept. of Struc. Mech., Chalmers Institute of Technology, Goteborg, Sweden, 1978.
14. J.R. Booker, and J.C. Small, "An Investigation of the Stability of Numerical Solutions of Biot's Equations of Consolidation", Int. Jour. Solids Struct., Vol. 11, 907-917, 1975.
15. P.A. Vermeer, and A. Verruijt, "An Accuracy Condition for Consolidation by Finite Elements", Int. Jour. Numer. Anal Methods in Geomechanics, Vol. 5, 1-14, 1981.
16. J.P. Carter, J.R. Booker, and J.C. Small, "The Analysis of Finite Elasto-Plastic Consolidation", Int.

Jour. Numer. Anal. Methods in Geomechanics, Vol. 3, 107-129, 1979.

17. L. Suklje, "Stress and Strain in Nonlinear Viscous Soils", Int. Jour. Numer. Anal. Methods in Geomechanics, Vol. 2, 129-158, 1978.

18. J.P. Carter, J.C. Small, and J.R. Booker, "A Theory of Finite Elastic Consolidation", Int. Jour. Solids Struct., Vol. 13, 467-478, 1977.

19. J.H. Siriwardane, and C.S. Desai, "Two Numerical Schemes for Nonlinear Consolidation", Int. Jour. Numer. Methods in Engrg., Vol. 17, 405=426, 1981.

20. A.B. Moussa, A Coupled Problem of Finite Deformation and Flow in Porous Media, Ph.D. Thesis, The Ohio State University, Columbus, Ohio, 1980.

21. G.J. Krause, Untersuchungen uber Numerische Verfahren fur Elastisch, porose Medien, Dr. Ing. Thesis, Technische Universitat, Berlin, West Germany, 1975.

22. G.J. Krause, "Finite Element Schemes for Porous Elastic Media", Proceedings, Amer. Soc, Civ. Engrs., Vol.104, Jour. Engrg. Mech. Div., 605-620, 1978.

23. P.K. Banerjee, and R. Butterfield, "Transient Flow Through Porous Elastic Media", Chapter 2, Developments in Boundary Element Methods-2, Eds. P.K. Banerjee, and R. P. Shaw, Applied Science Publishers, England, 1981.

24. T. Kuroki, T. Ito, and K. Onishi, "Boundary Element Method in Biot's Linear Consolidation", App. Math. Modelling, Vol. 6, 105-110, 1982.

25, Y. Yokoo, K. Yamagata, and H. Nagaonka, "Finite Element Method Applied to Biot's Consolidation Theory", Soils and Foundations, Vol. 11, 29-46, 1971.

26. R. Buchmaier, Personal communications, 1980, 1981.

27. P.A. Vermeer, Personal communication, 1980.

28. M.A. Biot, "General Theory of Three-Dimensional Consolidation", Jour. App. Phy., Vol 12, 155-164, 1941.

29. R.S. Sandhu, Finite Element Analysis of Coupled Deformation and Fluid Flow in Porous Media, NATO Advanced Study Institute, Vimeiro, Portugal, 1981.

30. R.S. Sandhu, Finite Element Analysis of Soil Consolidation, Report OSURF-3570-3 to National Science Foundation, Dept. of Civ. Engrg., The Ohio State University, Columbus, Ohio, 1976.

31. T.J.R. Hughes, and J.E. Akin, "Techniques for Developing 'Special' Finite Element Shape Functions with Particular Reference to Singularities", Int. Jour. Numer. Methods in Engrg., Vol. 15, 733-751, 1980.

32. S.C. Lee, Special Finite Elements for Analysis of Soil Consolidation, M.S. Thesis, The Ohio State University, Columbus, Ohio, 1982.

33. C.T. Hwang, N.R. Morgenstern, and D.W. Murray, "On Solution of Plane Strain Consolidation Problems by Finite Element Methods", Canadian Geotech. Jour., Vol. 8, 109-118, 1971.

34. S.A. Asproudas, and C.S. Desai, Analysis and Applications of a Finite Element Procedure for

Consolidation, Dept. of Civ. Engrg., Virginia Polytech. Inst. and State University, Blacksburg, Virginia, 1975.

35. H.L. Martin, Implementation and Comparison of the Biot and Terzaghi-Rendulic Theories of Consolidation, Ph. D. Thesis, University of Colorado, Boulder, Colorado, 1976.

36. S. Valliappan, I.K. Lee, and P. Boonlualohr, "Finite Element Analysis of Consolidation Problems", in Finite Element Methods in Flow Problems, Eds. J.T. Oden. O.C. Zienkiewicz, R. Gallagher, and C. Taylor, University of Alabama at Huntsville Press, Huntsville, Alabama, 1974.

37. Y. Yokoo, K. Yamagata, and H. Nagaonka, "Finite Element Analysis of Consolidation Following Undrained Deformation", Soils and Foundations, Vol. 11, 37-58, 1971.

38. M. Masseira, and M.R. Soulie, Etude par elements finis des deformations non-draineesdans un milieu poreux, Proceedings, Fifth Canadian Congress of App. Mech., Fredericton, 114-115, 1975.

39. J.T. Christian, and J.W. Boehmer, "Plane Strain Consolidation by Finite Elements", Proceedings, Amer. Soc. Civ. Engrs., Vol. 96, Jour. Soil Mech. Found. Div., 1435-1457, 1970.

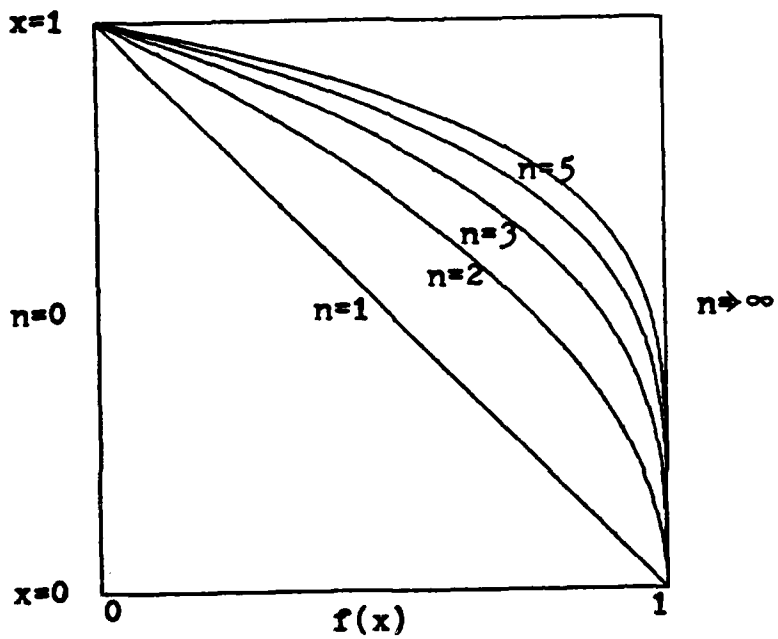

FIGURE 1. FUNCTION $f(x) = 1 - x^n$

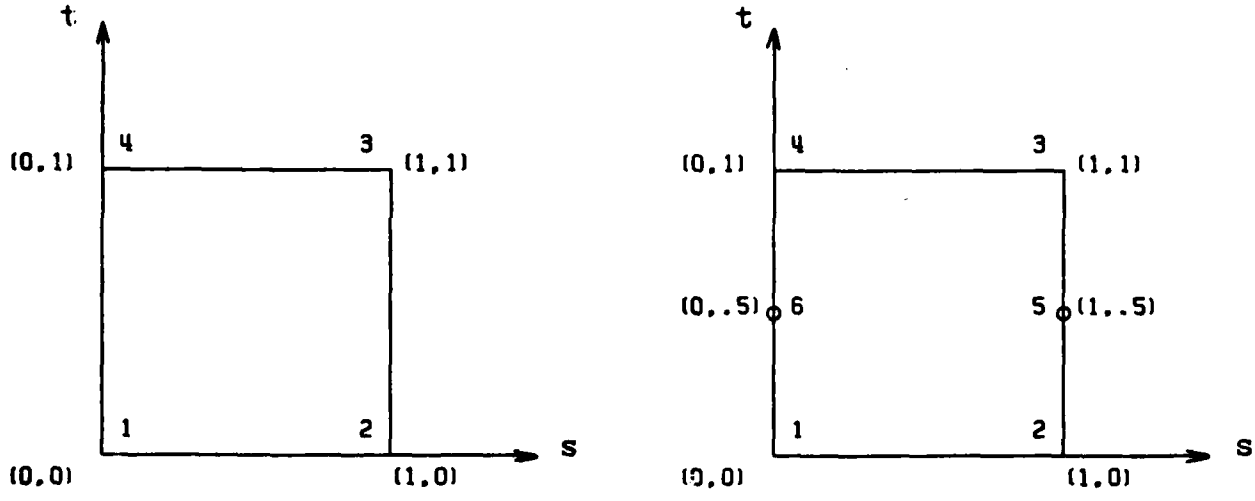

a. 8-4 ELEMENT

b. 8-6 ELEMENT

FIGURE 2. SINGULARITY ELEMENT - SINGULARITY ALONG AXIS t AT EDGE 3-4

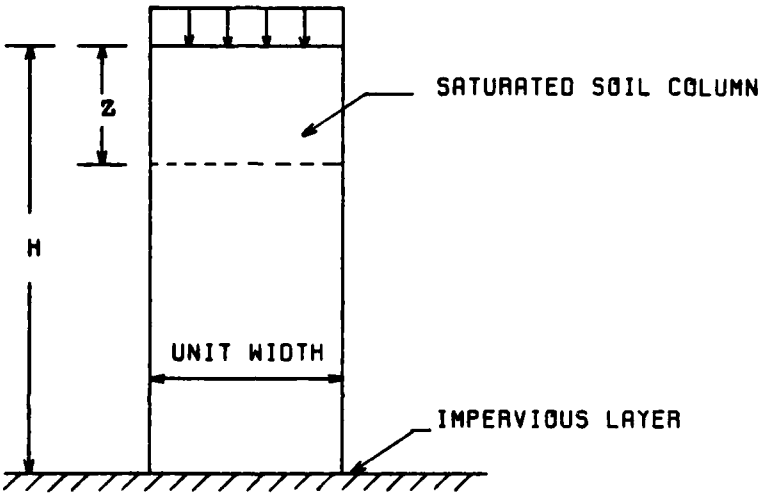

FIGURE 3. CONSOLIDATING SOIL COLUMN - TERZAGHI'S PROBLEM

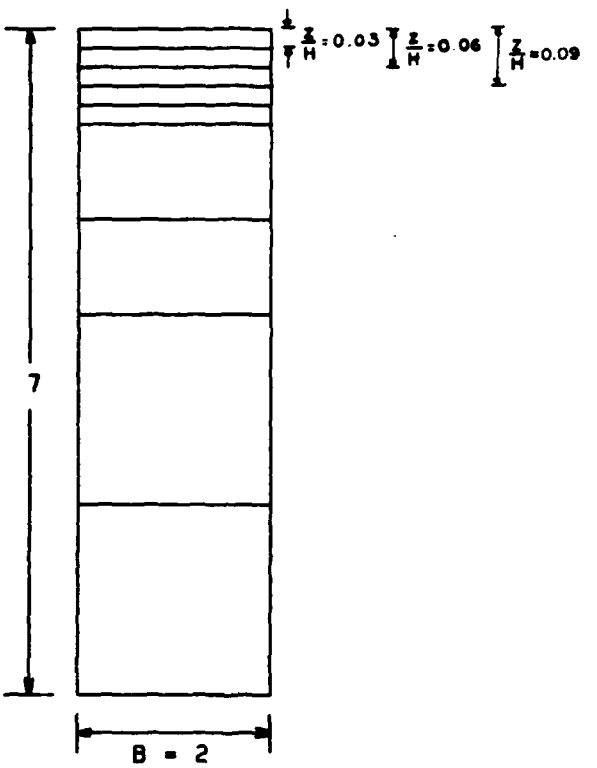

FIGURE 4. FINITE ELEMENT MESH (8-4 ELEMENT)

LOCATION = 0.03 H

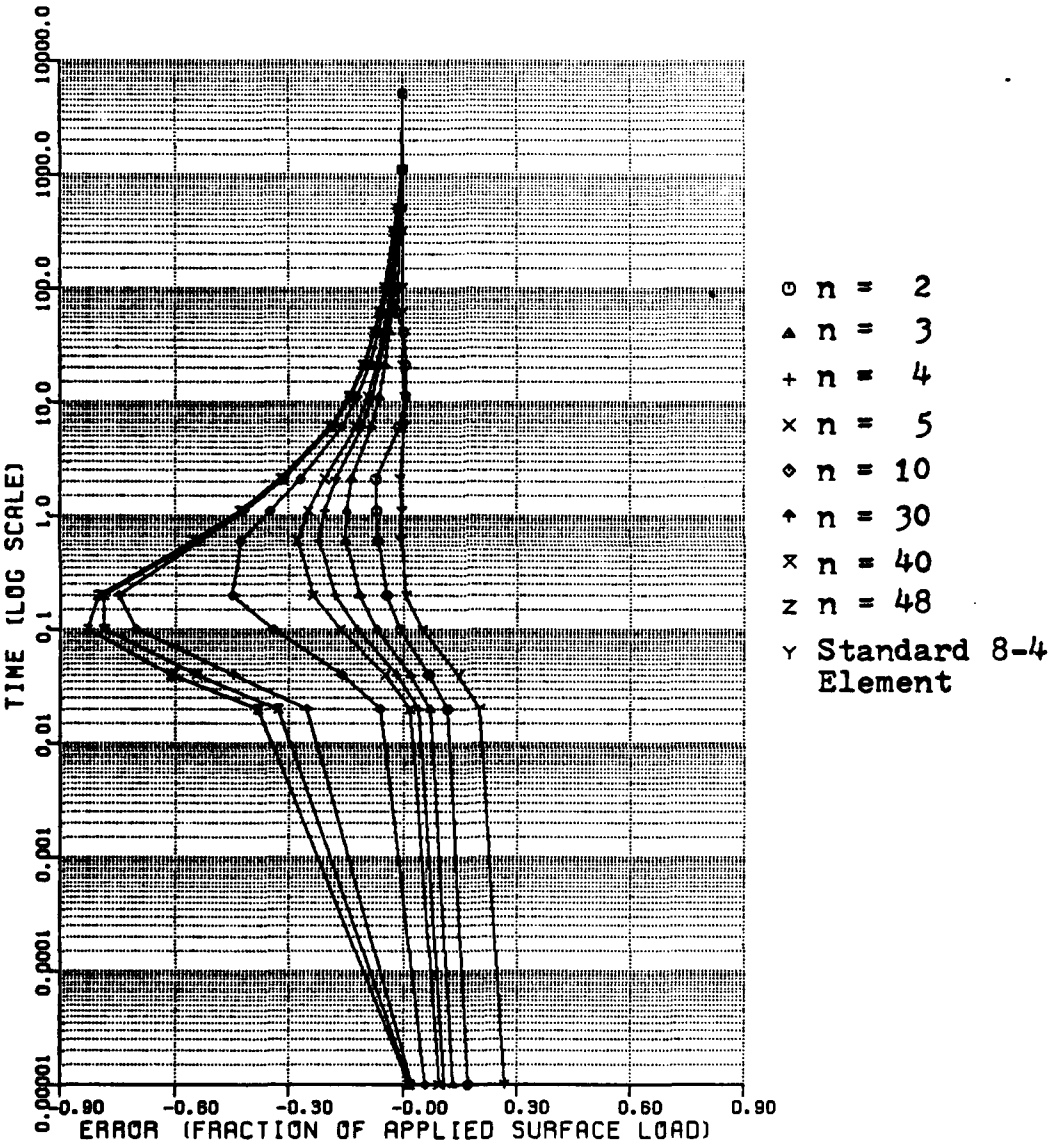

FIGURE 5A DISTRIBUTION OF THE 'RELATIVE' ERROR IN PORE PRESSURE (Special 8-4 Element , Shape Function based on $f(x) = 1-x^n$)

TABLE 1A PORE PRESSURE AT 0.03H BELOW THE SURFACE USING SPECIAL 8-4 ELEMENT (shape function based on $f(x)= 1-x^n$)

τ \ n	2	3	4	5	10	PS84	EXACT
0.0	1.170131	1.130651	1.108655	1.093963	1.057777	1.267909	1.000000
0.000021	1.114712	1.070553	1.041118	1.018195	0.938806	1.200800	0.999990
0.000042	1.064806	1.016346	0.980464	0.950565	0.837148	1.141744	0.998177
0.000105	0.941145	0.881873	0.831388	0.786560	0.610515	1.001348	0.951382
0.000210	0.792353	0.720632	0.656167	0.598764	0.388006	0.842692	0.836802
0.000630	0.513842	0.429347	0.359709	0.304161	0.153485	0.572994	0.579220
0.001154	0.379110	0.301061	0.242951	0.200460	0.100448	0.443835	0.447879
0.002204	0.262101	0.199028	0.156858	0.128295	0.066048	0.324711	0.333044
0.006402	0.188499	0.116573	0.092049	0.075733	0.039738	0.200795	0.199339
0.011650	0.155558	0.085684	0.067517	0.055513	0.029146	0.150597	0.148478
0.022146	0.115044	0.059339	0.046695	0.038386	0.020185	0.106004	0.107989
0.043137	0.080045	0.043038	0.033894	0.027883	0.014696	0.077033	0.077490
0.064128	0.047871	0.035494	0.027956	0.023002	0.012129	0.063605	0.063587
0.106111	0.037259	0.027615	0.021749	0.017895	0.009439	0.049568	0.049446
0.316023	0.019706	0.014555	0.011440	0.009400	0.004944	0.026345	0.026243
0.525936	0.011487	0.008430	0.006599	0.005408	0.002828	0.015482	0.015604
1.155674	0.002294	0.001652	0.001279	0.001040	0.000534	0.003166	0.003299
5.353927	0.000001	0.000001	0.000001	0.0	0.0	0.000001	0.0

TABLE 1B PORE PRESSURE AT 0.03H BELOW THE SURFACE USING SPECIAL 8-4 ELEMENT (shape function based on $f(x)= 1-x^n$)

τ \ n	30	40	48	PS84	EXACT
0.0	1.023126	1.017748	1.014936	1.267909	1.000000
0.000021	0.746686	0.673083	0.620172	1.200800	0.999990
0.000042	0.552640	0.454235	0.388960	1.141744	0.998177
0.000105	0.250262	0.167274	0.123897	1.001348	0.951382
0.000210	0.089270	0.052175	0.038249	0.842692	0.836802
0.000630	0.044371	0.032694	0.027008	0.572994	0.579220
0.001154	0.031994	0.023835	0.019794	0.443835	0.447879
0.002204	0.022220	0.016665	0.013887	0.324711	0.333044
0.006402	0.013583	0.010215	0.008523	0.200795	0.199339
0.011650	0.009982	0.007510	0.006268	0.150597	0.148478
0.022146	0.006934	0.005219	0.004357	0.106004	0.107989
0.043137	0.005059	0.003809	0.003181	0.077033	0.077490
0.064128	0.004178	0.003146	0.002627	0.063605	0.063587
0.106111	0.003252	0.002449	0.002045	0.049568	0.049446
0.316023	0.001700	0.001280	0.001069	0.026345	0.026243
0.525936	0.000968	0.000729	0.000608	0.015482	0.015604
1.155674	0.000181	0.000136	0.000113	0.003166	0.003299
5.353927	0.0	0.0	0.0	0.000001	0.0

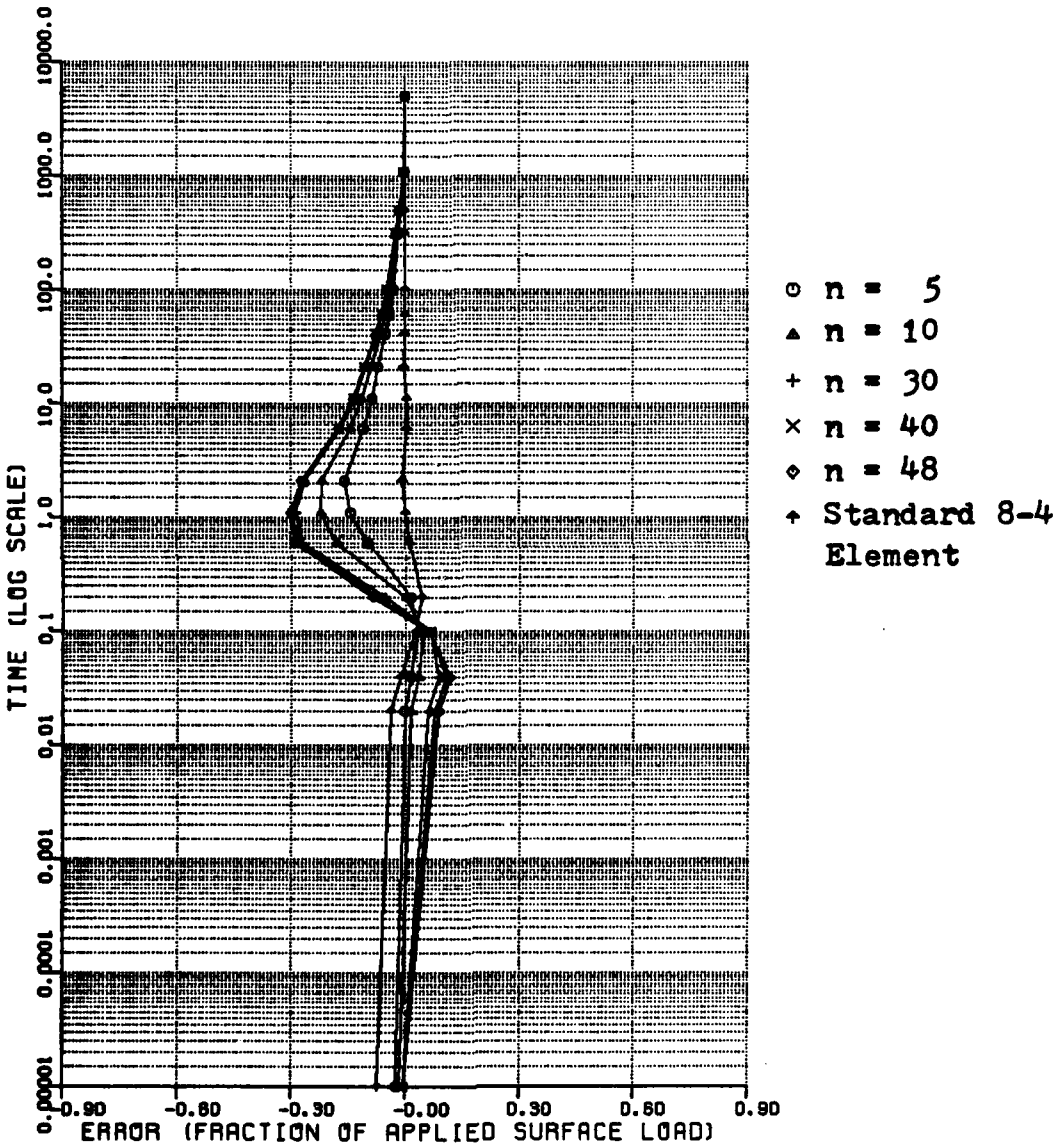

FIGURE 5B DISTRIBUTION OF THE 'RELATIVE' ERROR IN PORE PRESSURE (Special 8-4 Element , Shape Function based on $f(x) = 1-x^n$)

TABLE 1C PORE PRESSURE AT 0.06H BELOW THE SURFACE USING SPECIAL 8-4 ELEMENT (shape function based on $f(x)= 1-x^n$)

τ \ n	5	10	30	40	48	PS84	EXACT
0.0	0.974832	0.984524	0.993806	0.995246	0.995999	0.928240	1.000000
0.000021	0.998811	1.016137	1.059583	1.076370	1.088422	0.961856	1.000000
0.000042	1.015374	1.035770	1.088679	1.106554	1.118104	0.987231	1.000000
0.000105	1.033625	1.046955	1.066386	1.065718	1.063237	1.028603	0.999920
0.000210	1.010454	0.994965	0.941461	0.922025	0.909920	1.037672	0.994710
0.000630	0.796477	0.716273	0.624666	0.611735	0.605259	0.904833	0.892633
0.001154	0.624158	0.546389	0.479378	0.470549	0.466117	0.767321	0.765628
0.002204	0.452515	0.393112	0.348481	0.342688	0.339777	0.603856	0.610575
0.006402	0.278089	0.243413	0.217492	0.214110	0.212407	0.390208	0.386430
0.011650	0.206155	0.180081	0.160799	0.158290	0.157028	0.296013	0.291858
0.022146	0.143926	0.125666	0.112279	0.110541	0.109667	0.210342	0.214009
0.043137	0.104869	0.091708	0.082056	0.080802	0.080171	0.153390	0.154251
0.064128	0.086609	0.075758	0.067802	0.066768	0.066248	0.126819	0.126772
0.106111	0.067453	0.059004	0.052812	0.052008	0.051603	0.098948	0.098701
0.316023	0.035460	0.030925	0.027619	0.027190	0.026975	0.052635	0.052433
0.525936	0.020402	0.017689	0.015730	0.015477	0.015350	0.030933	0.031177
1.155674	0.003923	0.003344	0.002936	0.002884	0.002858	0.006326	0.006592
5.353927	0.000002	0.000002	0.000002	0.000002	0.000002	0.000002	0.0

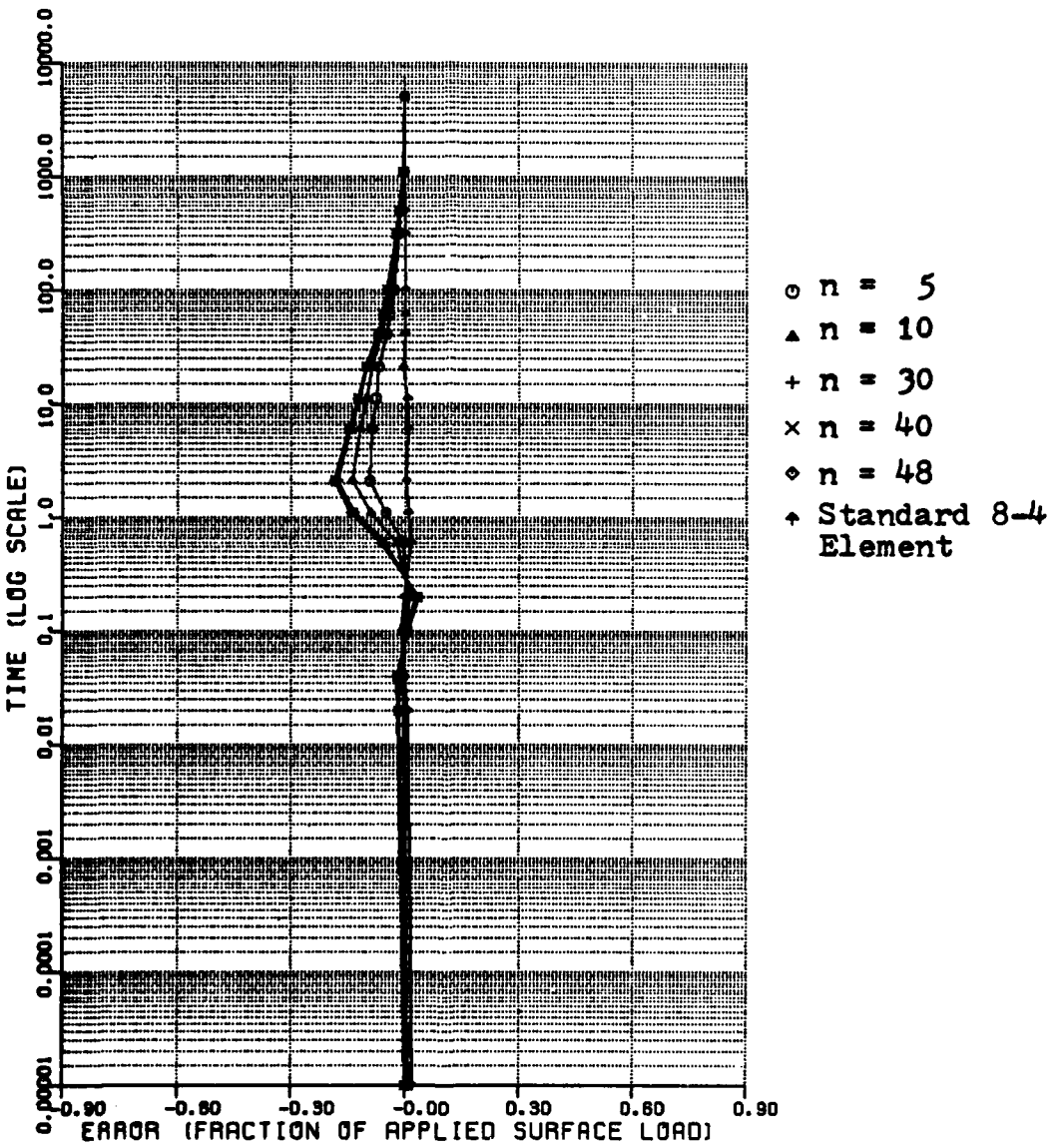

FIGURE 5C DISTRIBUTION OF THE 'RELATIVE' ERROR IN PORE PRESSURE (Special 8-4 Element, Shape Function based on $f(x) = 1-x^n$)

TABLE 1D PORE PRESSURE AT 0.09H BELOW THE SURFACE USING SPECIAL 8-4 ELEMENT (shape function based on $f(x)= 1-x^{n}$)

τ \ n	5	10	30	40	48	PS84	EXACT
0.0	1.006721	1.004133	1.001654	1.001270	1.001068	1.019164	1.000000
0.000021	0.999490	0.995784	0.986075	0.982287	0.979572	1.006598	1.000000
0.000042	0.995666	0.992303	0.983125	0.980155	0.978326	0.998586	1.000000
0.000105	0.995845	0.996964	1.002224	1.005213	1.007485	0.991172	1.000000
0.000210	1.005906	1.012433	1.028092	1.032177	1.034364	0.998152	0.999971
0.000630	0.979524	0.962368	0.931896	0.925858	0.922648	1.000281	0.984274
0.001154	0.874978	0.835686	0.793413	0.787116	0.783894	0.934463	0.925537
0.002204	0.710177	0.664587	0.626550	0.621454	0.618882	0.805508	0.803293
0.006402	0.464070	0.432687	0.408510	0.405308	0.403693	0.558574	0.551235
0.011650	0.349475	0.324596	0.305883	0.303428	0.302191	0.431559	0.425563
0.022146	0.247241	0.229218	0.215913	0.214180	0.213308	0.311395	0.316197
0.043137	0.180941	0.167925	0.158344	0.157097	0.156470	0.228410	0.229575
0.064128	0.149681	0.138920	0.131008	0.129979	0.129461	0.189257	0.189157
0.106111	0.116753	0.108343	0.102170	0.101368	0.100964	0.147951	0.147578
0.316023	0.061441	0.056837	0.053476	0.053040	0.052821	0.078814	0.078515
0.525936	0.035352	0.032512	0.030457	0.030192	0.030058	0.046320	0.046688
1.155674	0.006798	0.006147	0.005686	0.005627	0.005597	0.009472	0.009871
5.353927	0.000004	0.000004	0.000004	0.000004	0.000004	0.000003	0.0

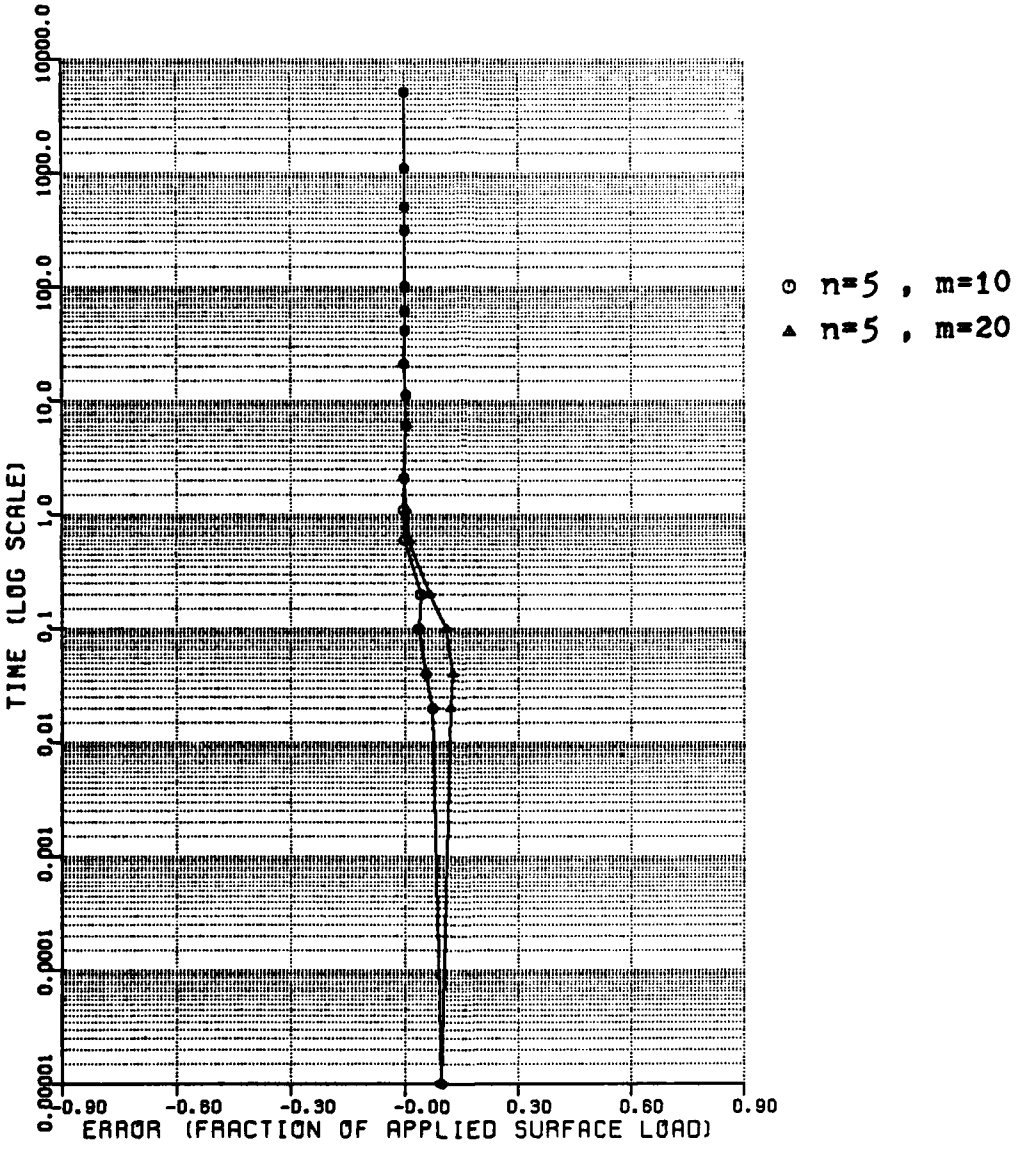

FIGURE 6A DISTRIBUTION OF THE 'RELATIVE' ERROR IN PORE PRESSURE (Special 8-4 Element , Shape Function based on $f(x)=1-ax-(1-a)x^n$, $a=1-e^{-mt}$)

LØCATIØN = 0.03 H

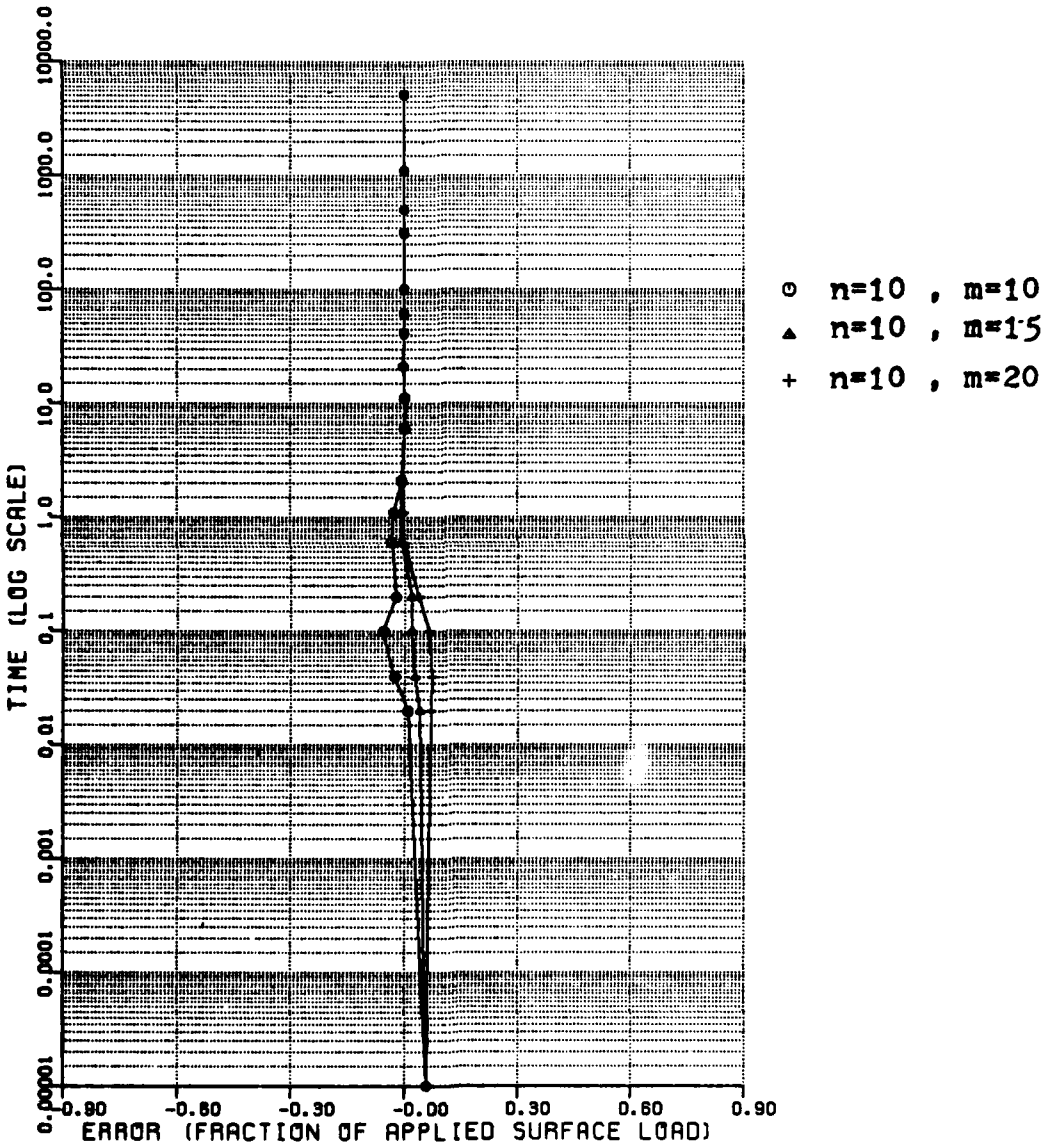

FIGURE 6B DISTRIBUTION OF THE 'RELATIVE' ERROR IN PORE PRESSURE (Special 8-4 Element , Shape Function based on $f(x)=1-ax-(1-a)x^n$, $a=1-e^{-mt}$)

TABLE 2A PORE PRESSURE AT 0.03H BELOW THE SURFACE USING SPECIAL 8-4 ELEMENT (shape function based on $f(x)= 1-ax-(1-a)x^{n}$, $a=1-e^{-mt}$)

τ \ n	5(10)	5(20)	10(10)	10(15)	10(20)	PS84	EXACT
0.0	1.094003	1.094003	1.057841	1.057841	1.057841	1.267909	1.000000
0.000021	1.073098	1.118886	1.009185	1.040397	1.068952	1.200800	0.999990
0.000042	1.052553	1.123325	0.971781	1.025187	1.069701	1.141744	0.998177
0.000105	0.988082	1.059807	0.894734	0.970205	1.015935	1.001348	0.951382
0.000210	0.878094	0.900921	0.813794	0.855717	0.873698	0.842692	0.836802
0.000630	0.578427	0.590181	0.545773	0.571991	0.579917	0.572994	0.579220
0.001154	0.442328	0.451749	0.420054	0.441547	0.446535	0.443835	0.447879
0.002204	0.330280	0.327879	0.326907	0.325920	0.326053	0.324711	0.333044
0.006402	0.201261	0.201484	0.200139	0.200736	0.201013	0.200795	0.199339
0.011650	0.150642	0.150903	0.150015	0.150512	0.150685	0.150597	0.148478
0.022146	0.106066	0.106112	0.105902	0.105998	0.106043	0.106004	0.107989
0.043137	0.077080	0.077083	0.077027	0.077042	0.077055	0.077033	0.077490
0.064128	0.063645	0.063637	0.063623	0.063617	0.063622	0.063605	0.063587
0.106111	0.049601	0.049588	0.049599	0.049581	0.049580	0.049568	0.049446
0.316023	0.026373	0.026353	0.026385	0.026356	0.026352	0.026345	0.026243
0.525936	0.015508	0.015488	0.015523	0.015492	0.015487	0.015482	0.015604
1.155674	0.003189	0.003168	0.003207	0.003175	0.003169	0.003166	0.003299
5.353927	0.000024	0.000002	0.000042	0.000009	0.000002	0.000001	0.0

LOCATION = 0.03 H

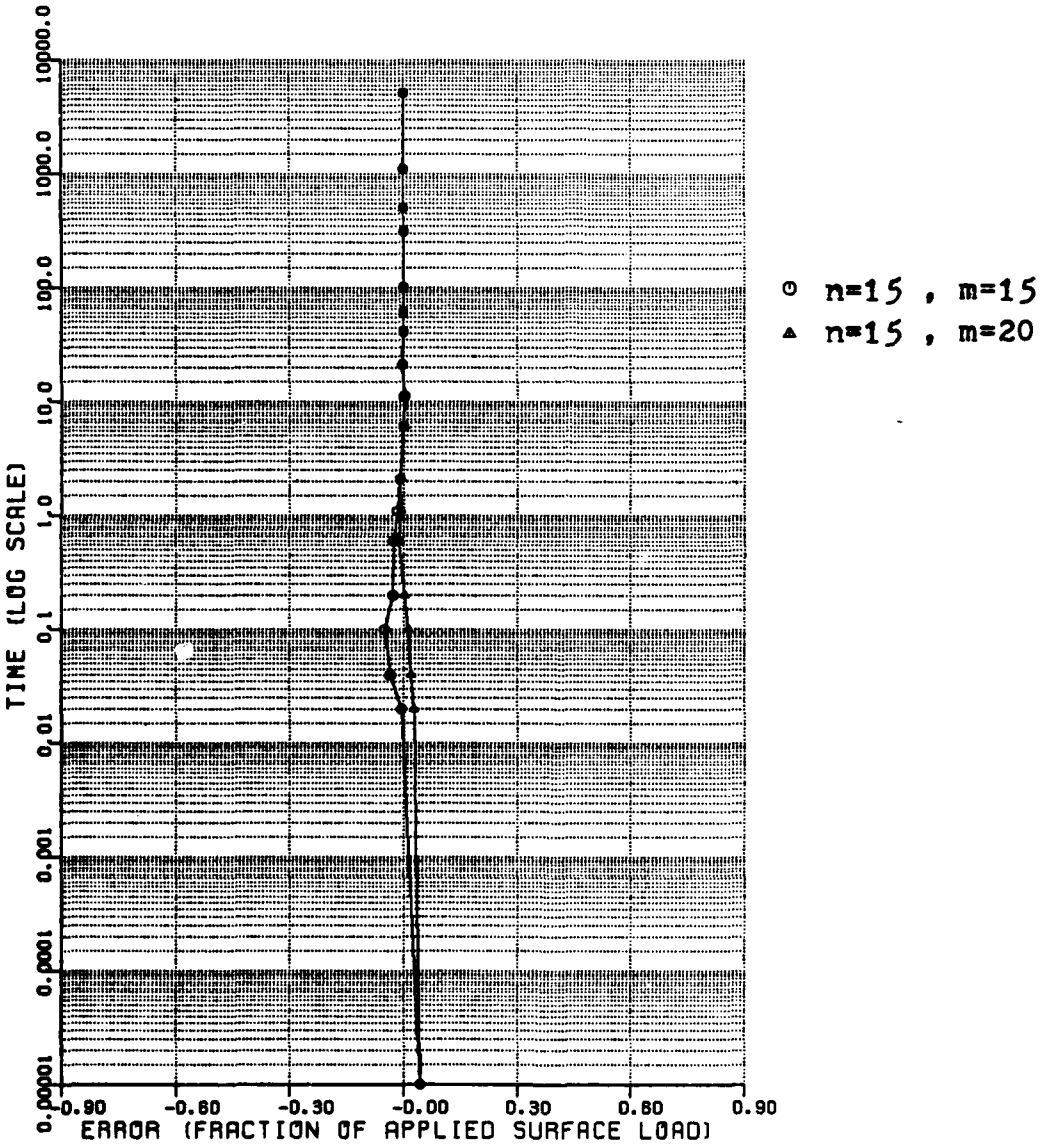

FIGURE 6C DISTRIBUTION OF THE 'RELATIVE' ERROR IN PORE PRESSURE (Special 8-4 Element , Shape Function based on $f(x)=1-ax-(1-a)x^n$, $a=1-e^{-mt}$)

TABLE 2B PORE PRESSURE AT 0.03H BELOW THE SURFACE USING SPECIAL 8-4 ELEMENT (shape function based on $f(x)= 1-ax-(1-a)x^{n}$, $a=1-e^{-mt}$)

τ \ n	15(15)	15(20)	30(30)	30(32.5)	30(40)	PS84	EXACT
0.0	1.042118	1.042118	1.023289	1.023289	1.023289	1.267909	1.000000
0.000021	0.995399	1.028047	0.997994	1.014278	1.058694	1.200800	0.999990
0.000042	0.964574	1.017581	0.989560	1.014011	1.067647	1.141744	0.998177
0.000105	0.902638	0.964336	0.931235	0.948475	0.985819	1.001348	0.951382
0.000210	0.809718	0.839484	0.802946	0.812334	0.833216	0.842692	0.836802
0.000630	0.554377	0.567545	0.555734	0.559309	0.567372	0.572994	0.579220
0.001154	0.432046	0.440343	0.434859	0.436646	0.440693	0.443835	0.447879
0.002204	0.323091	0.323857	0.321253	0.321900	0.323410	0.324711	0.333044
0.006402	0.199998	0.200461	0.199926	0.200094	0.200478	0.200795	0.199339
0.011650	0.150160	0.150431	0.150206	0.150284	0.150460	0.150597	0.148478
0.022146	0.105891	0.105962	0.105887	0.105911	0.105968	0.106004	0.107989
0.043137	0.077000	0.077023	0.076991	0.077001	0.077024	0.077033	0.077490
0.064128	0.063594	0.063603	0.063583	0.063589	0.063602	0.063605	0.063587
0.106111	0.049571	0.049571	0.049561	0.049564	0.049570	0.049568	0.049446
0.316023	0.026355	0.026349	0.026345	0.026345	0.026347	0.026345	0.026243
0.525936	0.015493	0.015486	0.015482	0.015483	0.015483	0.015482	0.015604
1.155674	0.003177	0.003169	0.003166	0.003166	0.003166	0.003166	0.003299
5.353927	0.000012	0.000003	0.000001	0.000001	0.000001	0.000001	0.0

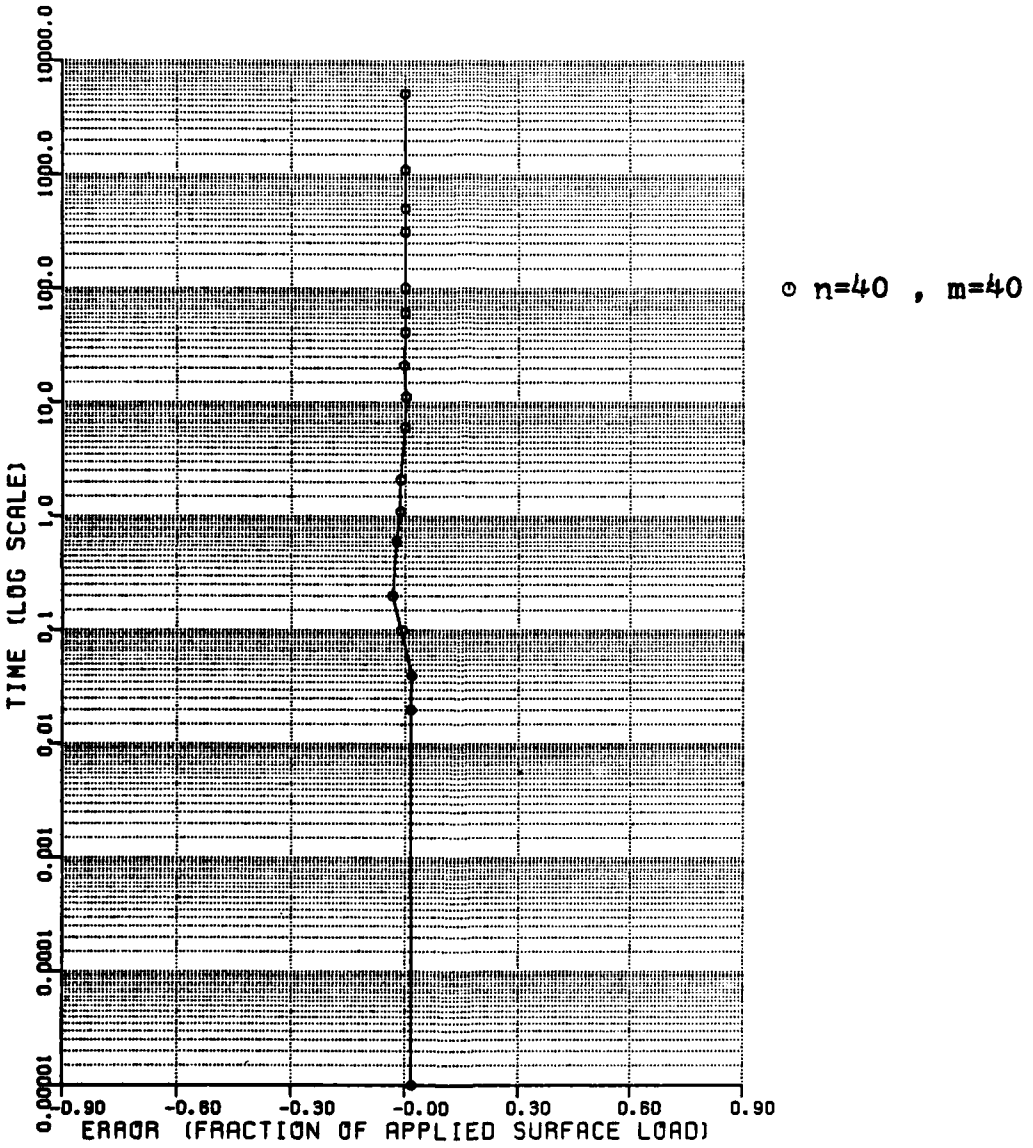

FIGURE 6E DISTRIBUTION OF THE 'RELATIVE' ERROR IN PORE PRESSURE (Special 8-4 Element , Shape Function based on $f(x)=1-ax-(1-a)x^n$, $a=1-e^{-mt}$)

LOCATION = 0.03 H

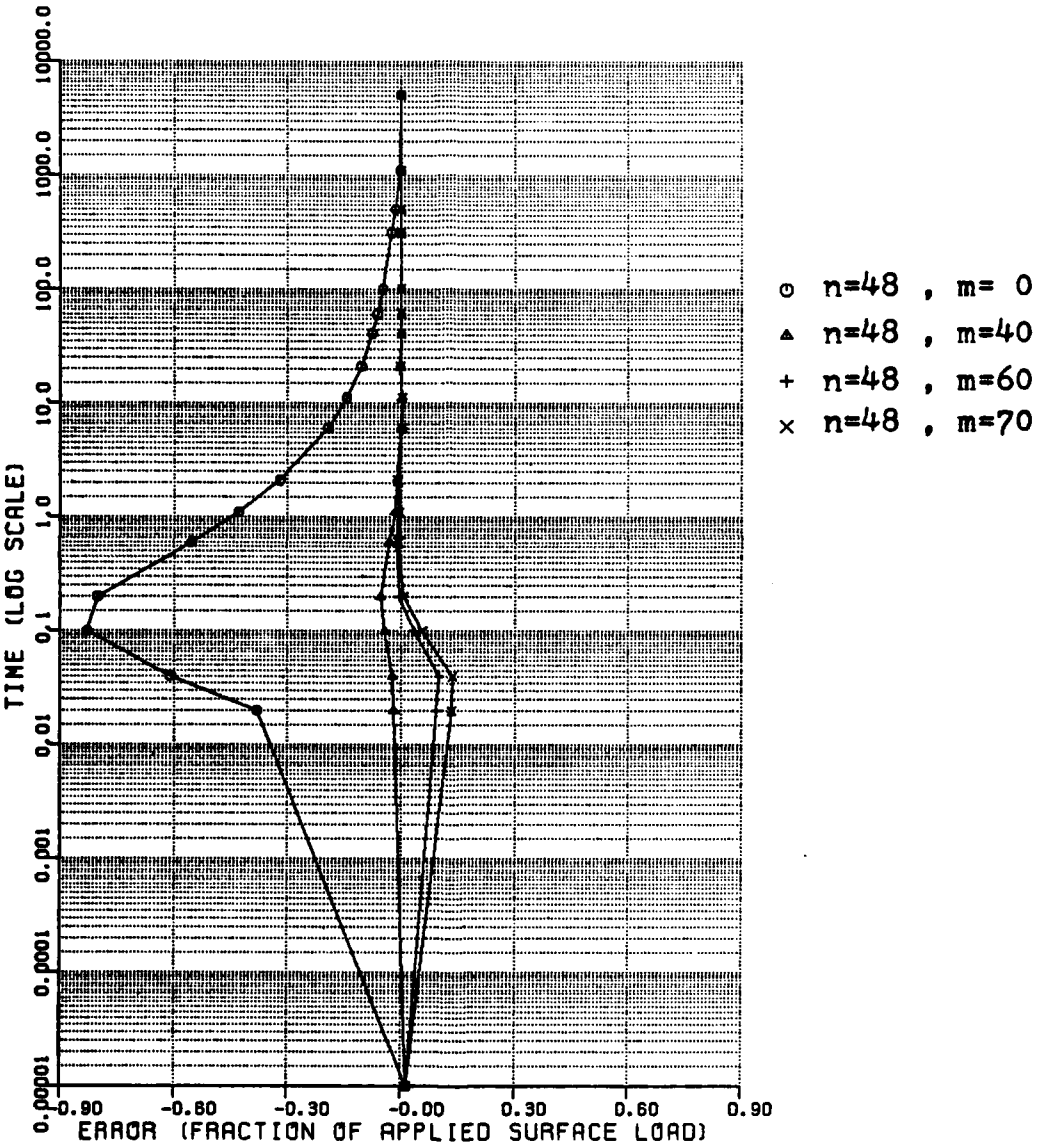

FIGURE 6F DISTRIBUTION OF THE 'RELATIVE' ERROR IN PORE PRESSURE (Special 8-4 Element , Shape Function based on $f(x)=1-ax-(1-a)x^n$, $a=1-e^{-mt}$)

TABLE 2C PORE PRESSURE AT 0.03H BELOW THE SURFACE USING SPECIAL 8-4 ELEMENT (shape function based on $f(x)= 1-ax-(1-a)x^{n}$, $a=1-e^{-mt}$)

τ \ n	40(40)	48(0)	48(40)	48(60)	48(70)	PS84	EXACT
0.0	1.017962	1.014936	1.015086	1.015161	1.015198	1.267909	1.000000
0.000021	1.014532	0.620172	0.980948	1.092554	1.132655	1.200800	0.999990
0.000042	1.015500	0.388960	0.975767	1.097860	1.132595	1.141744	0.998177
0.000105	0.942617	0.123897	0.909663	0.987630	1.007453	1.001348	0.951382
0.000210	0.804845	0.038249	0.783207	0.831992	0.845001	0.842692	0.836802
0.000630	0.557130	0.027008	0.549322	0.567735	0.572695	0.572994	0.579220
0.001154	0.435640	0.019794	0.431789	0.440995	0.443488	0.443835	0.447879
0.002204	0.321520	0.013887	0.320081	0.323563	0.324513	0.324711	0.333044
0.006402	0.200008	0.008523	0.199649	0.200521	0.200758	0.200795	0.199339
0.011650	0.150246	0.006268	0.150083	0.150480	0.150588	0.150597	0.148478
0.022146	0.105899	0.004357	0.105847	0.105974	0.106009	0.106004	0.107989
0.043137	0.076996	0.003181	0.076975	0.077026	0.077040	0.077033	0.077490
0.064128	0.063586	0.002627	0.063574	0.063604	0.063612	0.063605	0.063587
0.106111	0.049562	0.002045	0.049556	0.049571	0.049575	0.049568	0.049446
0.316023	0.026345	0.001069	0.026343	0.026347	0.026348	0.026345	0.026243
0.525936	0.015482	0.000608	0.015481	0.015484	0.015484	0.015482	0.015604
1.155674	0.003166	0.000113	0.003166	0.003166	0.003166	0.003166	0.003299
5.353927	0.000001	0.0	0.000001	0.000001	0.000001	0.000001	0.0

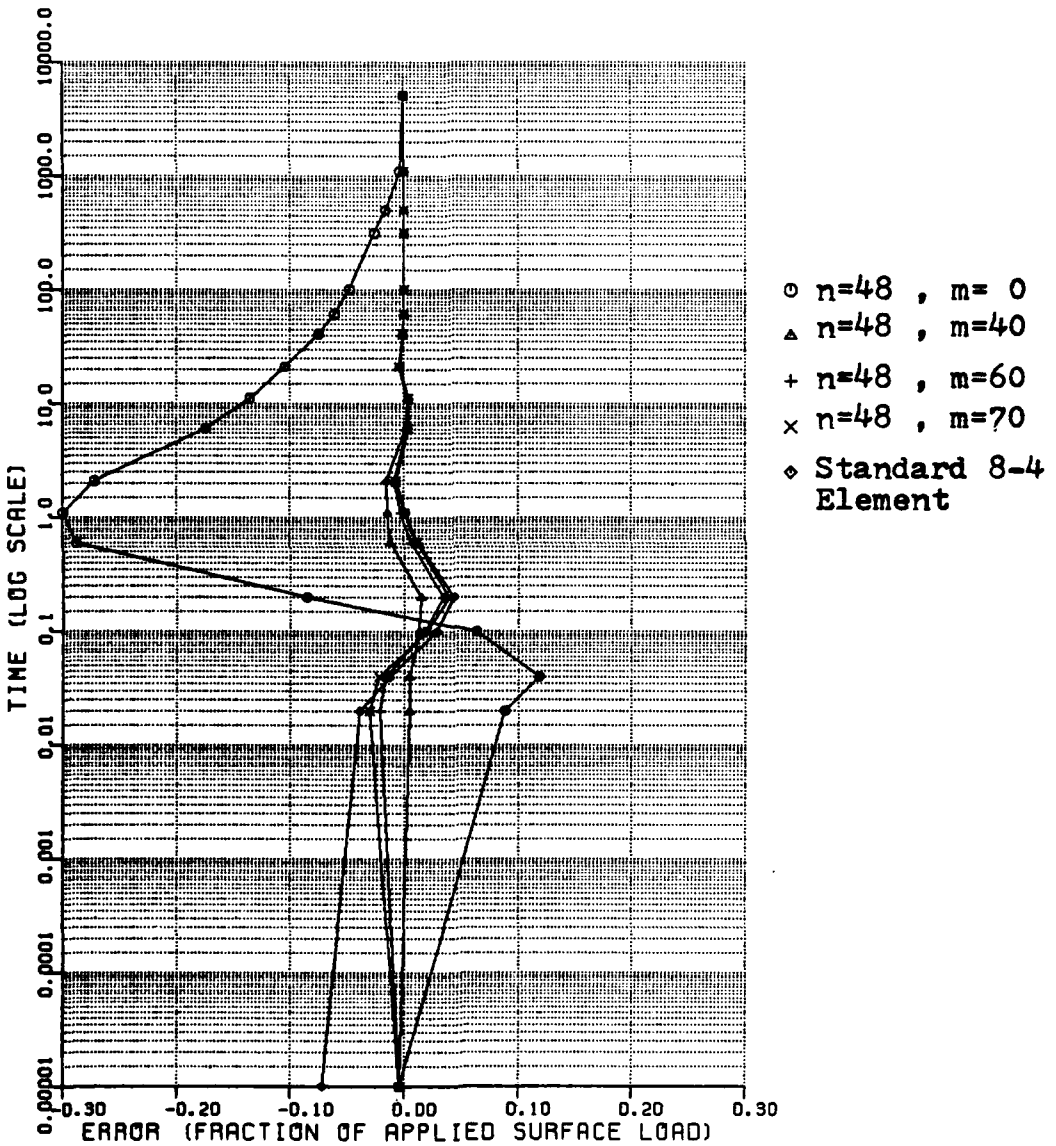

FIGURE 6G DISTRIBUTION OF THE 'RELATIVE' ERROR IN PORE PRESSURE (Special 8-4 Element , Shape Function based on $f(x)=1-ax-(1-a)x^n$, $a=1-e^{-mt}$)

TABLE 2D PORE PRESSURE AT 0.06H BELOW THE SURFACE USING SPECIAL 8-4 ELEMENT (shape function based on $f(x)=1-ax-(1-a)x^n, a=1-e^{-mt}$)

τ \ n	48(0)	48(40)	48(60)	48(70)	PS84	EXACT
0.0	0.995999	0.995959	0.995939	0.995929	0.928240	1.000000
0.000021	1.088422	1.004643	0.979156	0.970138	0.961856	1.000000
0.000042	1.118104	1.004644	0.983891	0.978662	0.987231	1.000000
0.000105	1.063237	1.013180	1.017936	1.019936	1.028603	0.999920
0.000210	0.909920	1.009910	1.028758	1.033940	1.037672	0.994720
0.000630	0.605259	0.880849	0.898977	0.903889	0.904833	0.892633
0.001154	0.466117	0.751469	0.763445	0.766693	0.767321	0.765628
0.002204	0.339777	0.595956	0.601889	0.603503	0.603856	0.610575
0.006402	0.212407	0.388061	0.389674	0.390113	0.390208	0.386430
0.011650	0.157028	0.295013	0.295769	0.295975	0.296013	0.291858
0.022146	0.109667	0.210017	0.210268	0.210337	0.210342	0.214009
0.043137	0.080171	0.153263	0.153366	0.153393	0.153390	0.154251
0.064128	0.066248	0.126748	0.126807	0.126823	0.126819	0.126772
0.106111	0.051603	0.098916	0.098945	0.098953	0.098948	0.098701
0.316023	0.026975	0.052627	0.052636	0.052638	0.052635	0.052433
0.525936	0.015350	0.030929	0.030933	0.030935	0.030933	0.031177
1.155674	0.002858	0.006325	0.006326	0.006326	0.006326	0.006592
5.353927	0.000002	0.000002	0.000002	0.000002	0.000002	0.0

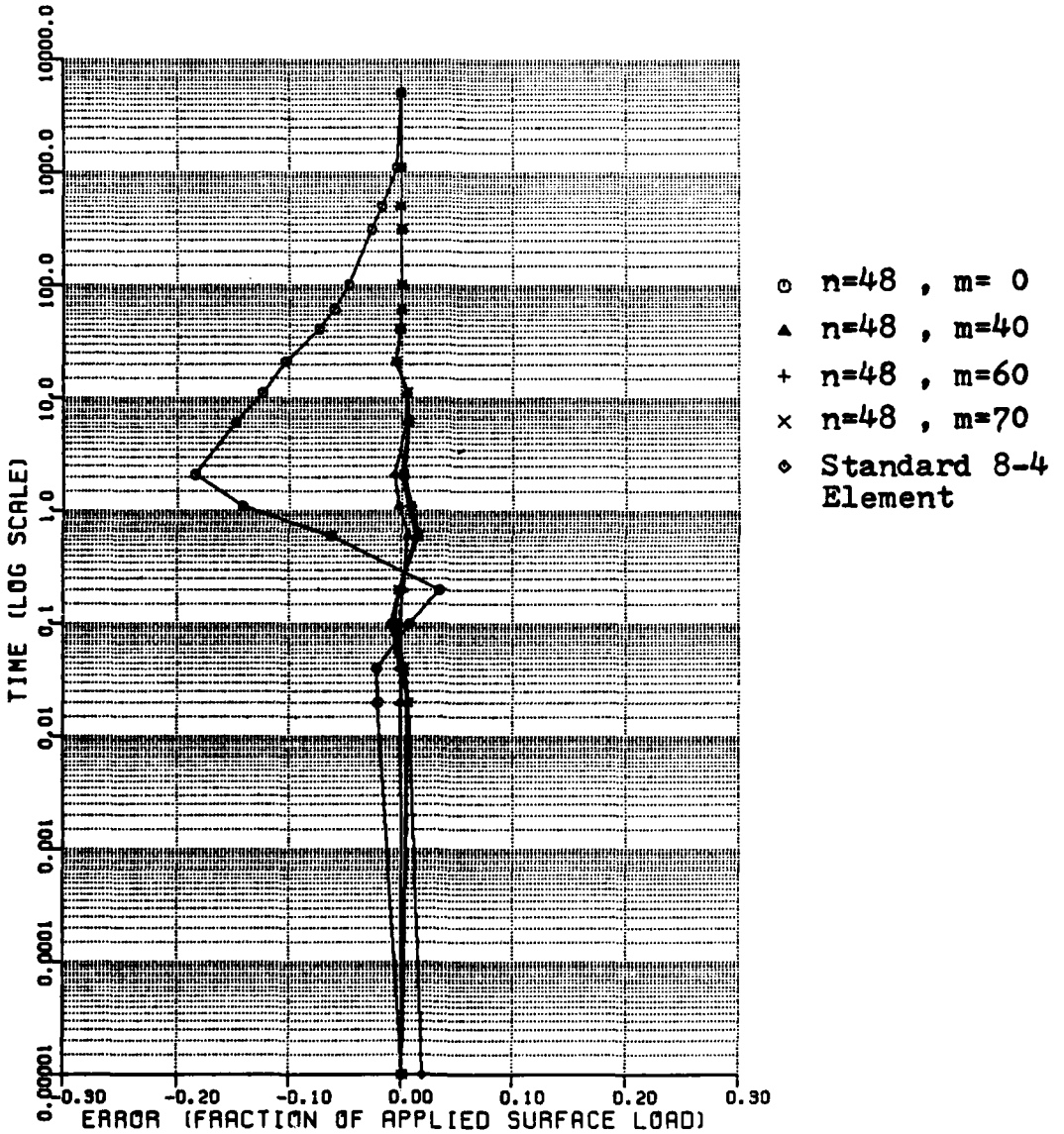

FIGURE 6H DISTRIBUTION OF THE 'RELATIVE' ERROR IN PORE PRESSURE (Special 8-4 Element , Shape Function based on $f(x)=1-ax-(1-a)x^n$, $a=1-e^{-mt}$)

TABLE 2E PORE PRESSURE AT 0.09H BELOW THE SURFACE USING SPECIAL 8-4 ELEMENT (shape function based on $f(x)=1-ax-(1-a)x^n$, $a=1-e^{-mt}$)

τ \ n	48(0)	48(40)	48(60)	48(70)	PS84	EXACT
0.0	1.001068	1.001079	1.001084	1.001087	1.019164	1.000000
0.000021	0.979572	0.998876	1.004634	1.006633	1.006598	1.000000
0.000042	0.978326	0.999168	1.002191	1.002744	0.998586	1.000000
0.000105	1.007485	0.998329	0.994278	0.993042	0.991172	1.000000
0.000210	1.034364	1.001542	0.998088	0.997265	0.998152	0.999971
0.000630	0.922648	0.990278	0.997382	0.999339	1.000281	0.984274
0.001154	0.783894	0.923017	0.931510	0.933823	0.934463	0.925537
0.002204	0.618882	0.797078	0.803401	0.805120	0.805508	0.803293
0.006402	0.403693	0.555743	0.557859	0.558435	0.558574	0.551235
0.011650	0.302191	0.430165	0.431211	0.431496	0.431559	0.425563
0.022146	0.213308	0.310912	0.311280	0.311380	0.311395	0.316197
0.043137	0.156470	0.228216	0.228367	0.228408	0.228410	0.229575
0.064128	0.129461	0.189147	0.189235	0.189259	0.189257	0.189157
0.1 6111	0.100964	0.147901	0.147944	0.147955	0.147951	0.147578
0.3.6023	0.052821	0.078801	0.078814	0.078817	0.078814	0.078515
0.525936	0.030058	0.046313	0.046320	0.046322	0.046320	0.046688
1.155674	0.005597	0.009471	0.009473	0.009473	0.009472	0.009871
5.353927	0.000004	0.000003	0.000003	0.000003	0.000003	0.0

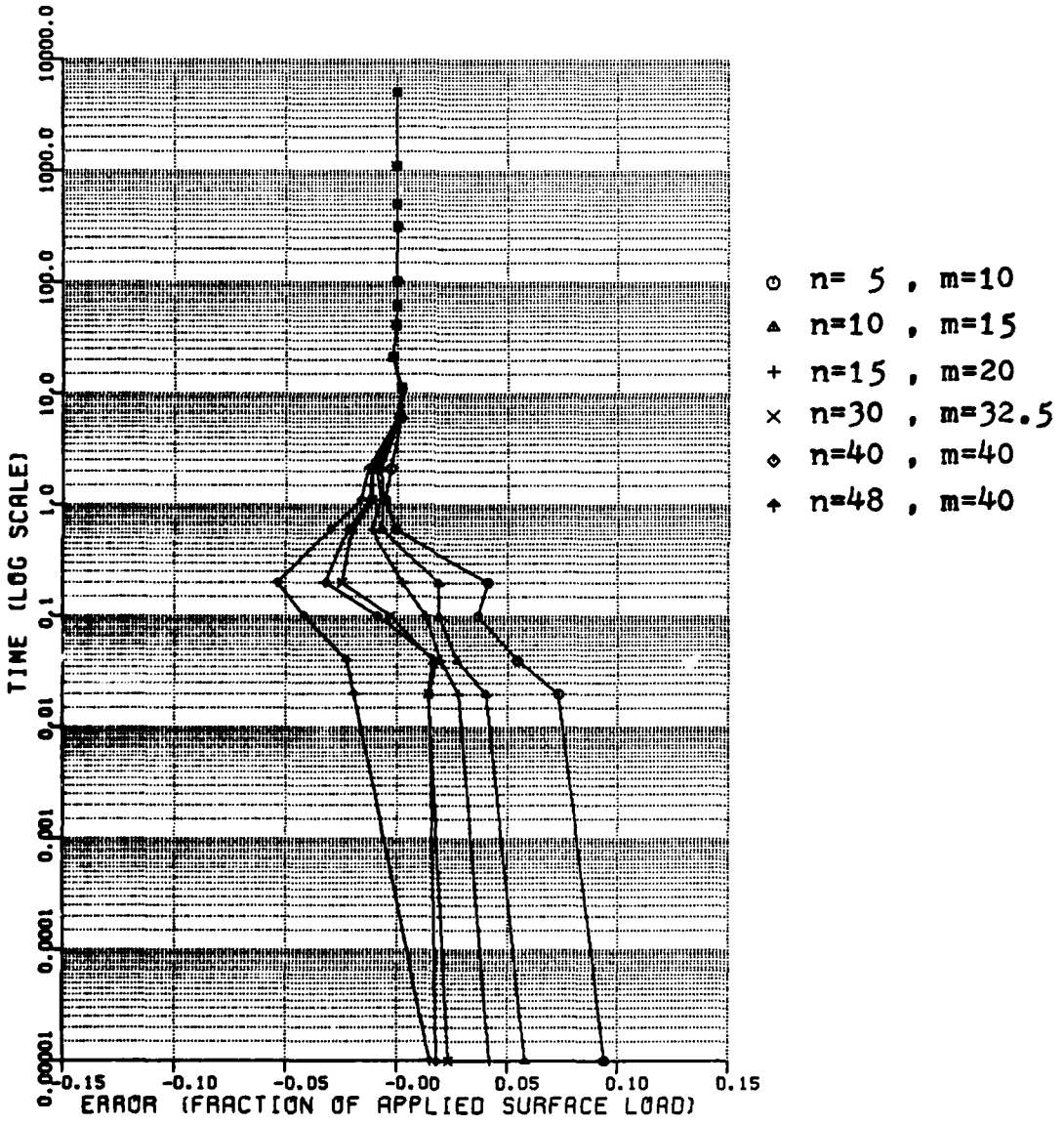

FIGURE 7 DISTRIBUTION OF THE 'RELATIVE' ERROR IN PORE PRESSURE (Special 8-4 Element , Shape Function based on $f(x)=1-ax-(1-a)x^n$, $a=1-e^{-mt}$)

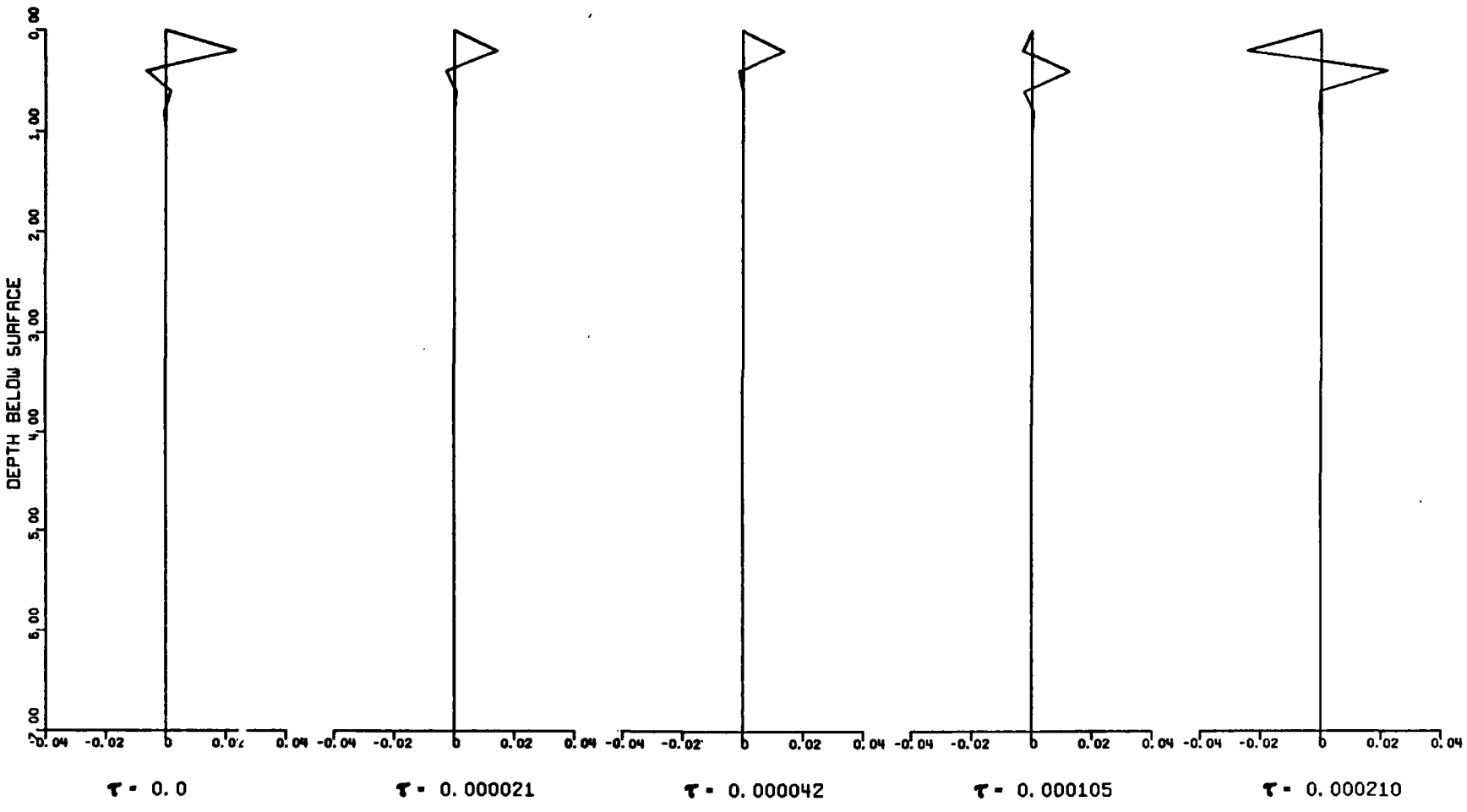

FIGURE 8A SPATIAL DISTRIBUTION OF THE 'RELATIVE' ERROR IN PORE PRESSURE

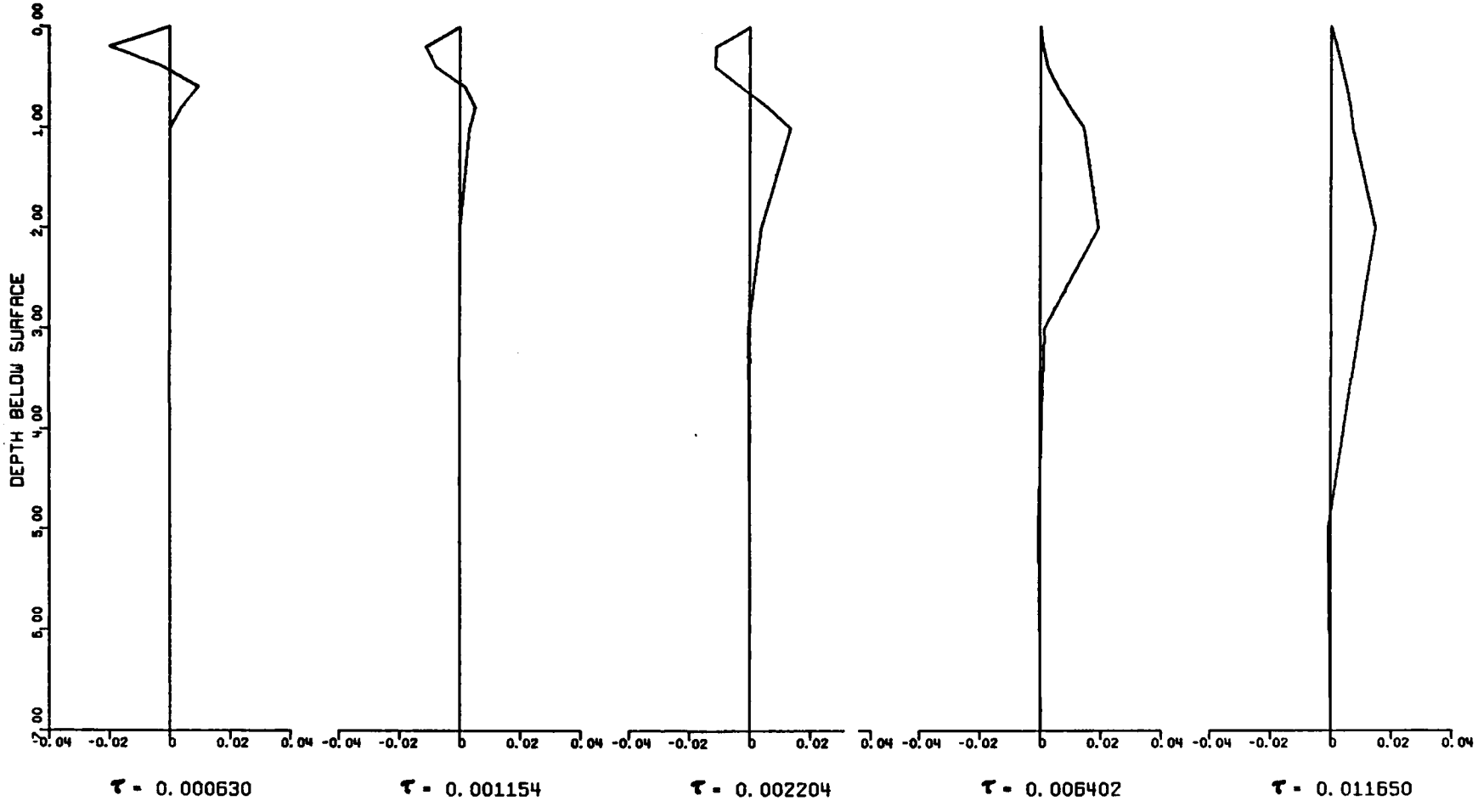

FIGURE 8B SPATIAL DISTRIBUTION OF THE 'RELATIVE' ERROR IN PORE PRESSURE

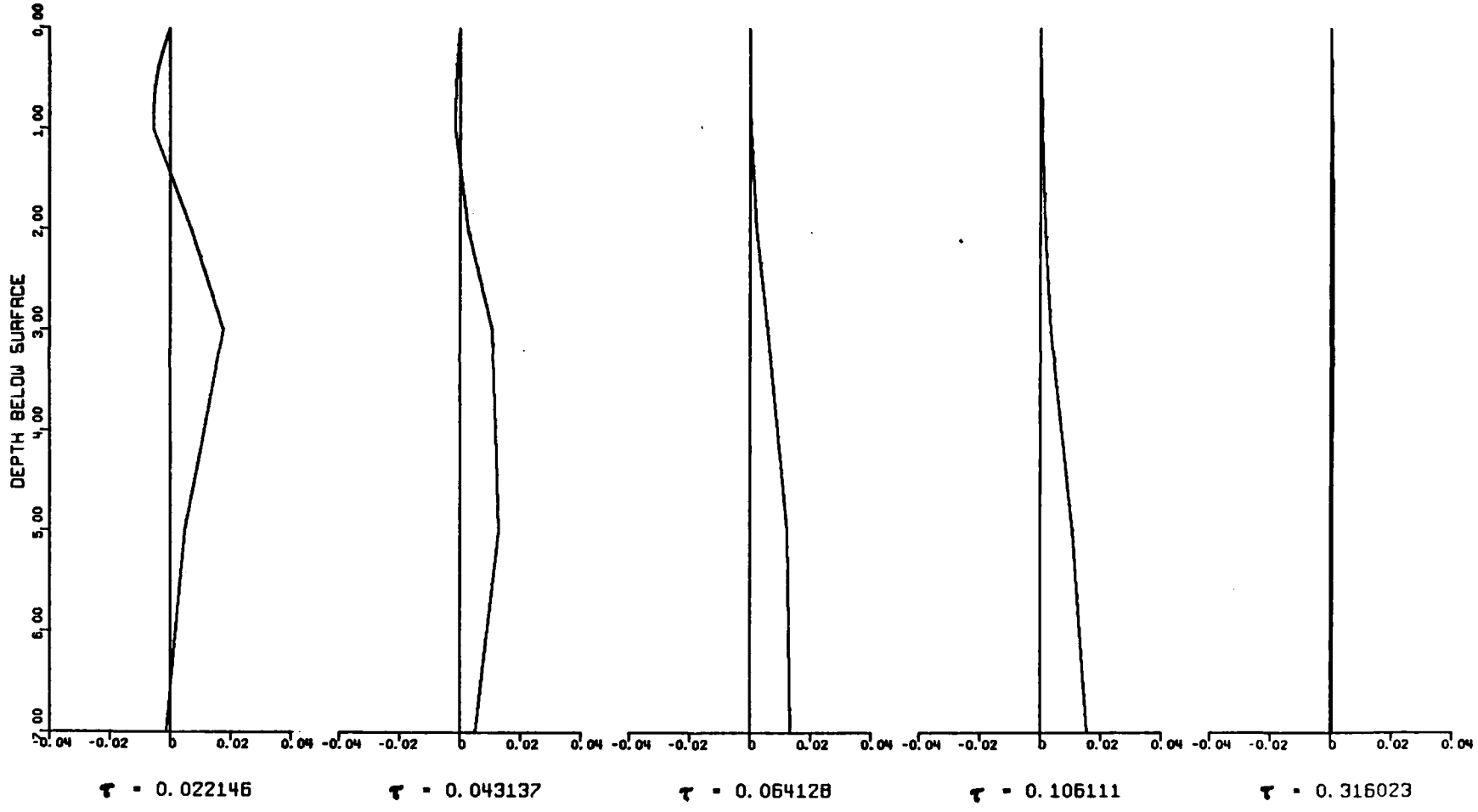

FIGURE 8C SPATIAL DISTRIBUTION OF THE 'RELATIVE' ERROR IN PORE PRESSURE

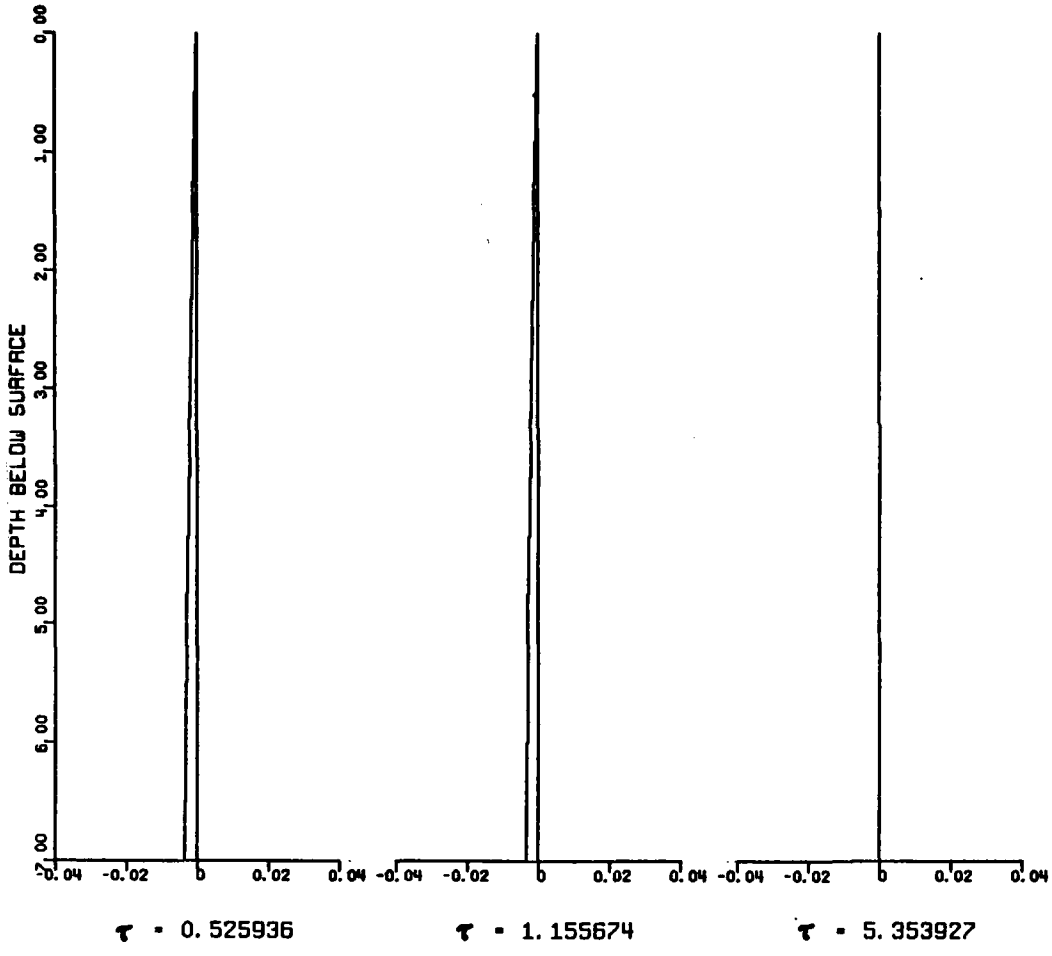

FIGURE 8D SPATIAL DISTRIBUTION OF THE 'RELATIVE' ERROR IN PORE PRESSURE

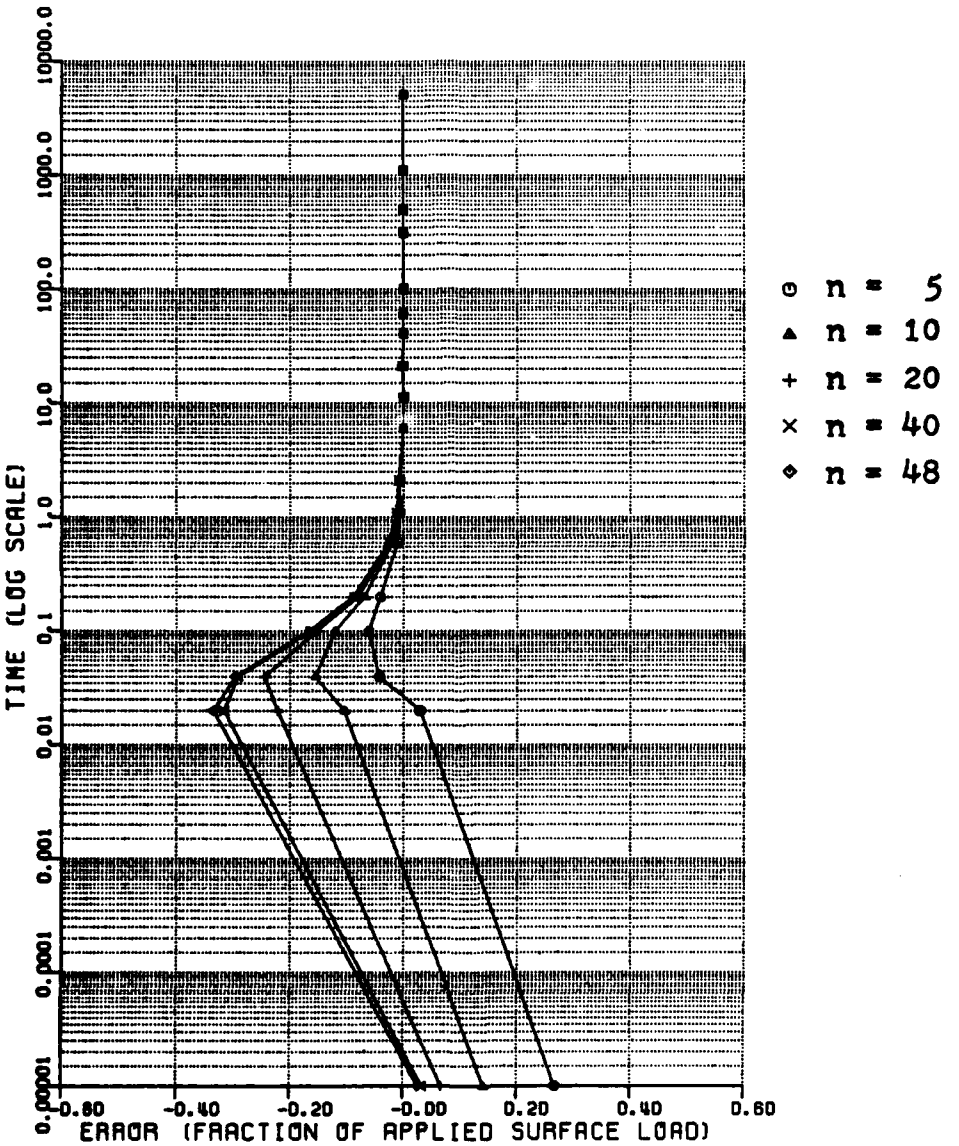

FIGURE 9A DISTRIBUTION OF THE 'RELATIVE' ERROR IN PORE PRESSURE (Special 8-6 Element , Shape Function based on $f(x)=a+bx+cx^n$)

TABLE 3A PORE PRESSURE AT 0.015H BELOW THE SURFACE USING SPECIAL 8-6 ELEMENT (shape function based on $f(x) = a + bx + cx^n$).

τ \ n	5	10	30	40	48	EXACT
0.0	1.266902	1.142116	1.067463	1.032518	1.026855	1.000000
0.000021	1.001748	0.869719	0.751484	0.655639	0.636879	0.972492
0.000042	0.839768	0.726080	0.635650	0.589132	0.584033	0.880962
0.000105	0.616285	0.555691	0.523077	0.510893	0.509106	0.675848
0.000210	0.473981	0.446725	0.434083	0.427634	0.426544	0.514321
0.000630	0.303446	0.294808	0.290424	0.288406	0.288080	0.312709
0.001154	0.229133	0.225501	0.223635	0.222756	0.222615	0.233757
0.002204	0.164511	0.163447	0.162888	0.162622	0.162579	0.170361
0.006402	0.100911	0.100663	0.100530	0.100467	0.100457	0.100463
0.011650	0.075534	0.075423	0.075363	0.075334	0.075329	0.074564
0.022146	0.053085	0.053049	0.053027	0.053017	0.053016	0.054119
0.043137	0.038556	0.038540	0.038530	0.038525	0.038525	0.038791
0.064128	0.031829	0.031819	0.031812	0.031809	0.031809	0.031819
0.106111	0.024800	0.024795	0.024791	0.024789	0.024789	0.024735
0.316023	0.013179	0.013177	0.013175	0.013175	0.013175	0.013125
0.525936	0.007745	0.007744	0.007743	0.007742	0.007742	0.007804
1.155674	0.001584	0.001584	0.001583	0.001583	0.001583	0.001650
5.353927	0.0	0.0	0.0	0.0	0.0	0.0

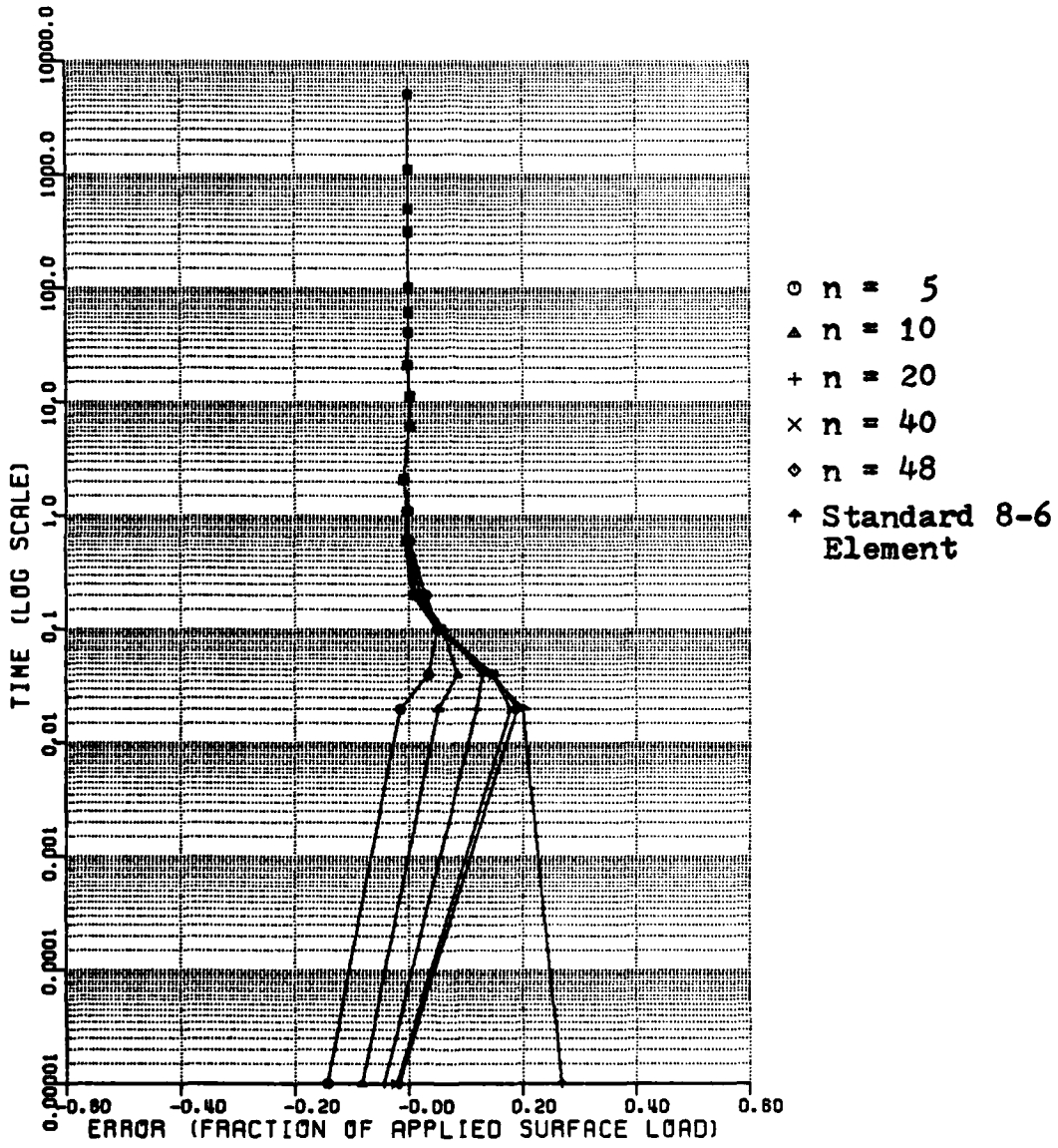

FIGURE 9B DISTRIBUTION OF THE 'RELATIVE' ERROR IN PORE PRESSURE (Special 8-6 Element , Shape Function based on $f(x) = a+bx+cx^n$)

TABLE 3B PORE PRESSURE AT 0.03H BELOW THE SURFACE USING SPECIAL 8-4 ELEMENT (shape function based on $f(x)= a+bx+cx^n$)

τ \ n	5	10	20	40	48	PS84	EXACT
0.0	0.857214	0.917763	0.956216	0.977583	0.981303	1.267909	1.000000
0.000021	0.985051	1.050856	1.119061	1.178775	1.190196	1.200800	0.999990
0.000042	1.033127	1.083665	1.127355	1.146638	1.147459	1.141744	0.998177
0.000105	1.001330	1.011821	1.011924	1.007458	1.006498	1.001348	0.951382
0.000210	0.866046	0.858566	0.850675	0.846677	0.846035	0.842692	0.836802
0.000630	0.580516	0.577369	0.575309	0.574175	0.573986	0.572994	0.579220
0.001154	0.446782	0.445502	0.444716	0.444301	0.444231	0.443835	0.447879
0.002204	0.325301	0.325052	0.324906	0.324829	0.324816	0.324711	0.333044
0.006402	0.200891	0.200861	0.200843	0.200833	0.200831	0.200795	0.199339
0.011650	0.150637	0.150629	0.150623	0.150621	0.150620	0.150597	0.148478
0.022146	0.106021	0.106021	0.106020	0.106020	0.106020	0.106004	0.107989
0.043137	0.077045	0.077045	0.077045	0.077045	0.077045	0.077033	0.077490
0.064128	0.063615	0.063614	0.063615	0.063614	0.063614	0.063605	0.063587
0.106111	0.049576	0.049576	0.049576	0.049576	0.049576	0.049568	0.049446
0.316023	0.026349	0.026349	0.026349	0.026349	0.026349	0.026345	0.026243
0.525936	0.015484	0.015484	0.015485	0.015484	0.015484	0.015482	0.015604
1.155674	0.003166	0.003166	0.003167	0.003167	0.003166	0.003166	0.003299
5.353927	0.000001	0.000001	0.000001	0.000001	0.000001	0.000001	0.0

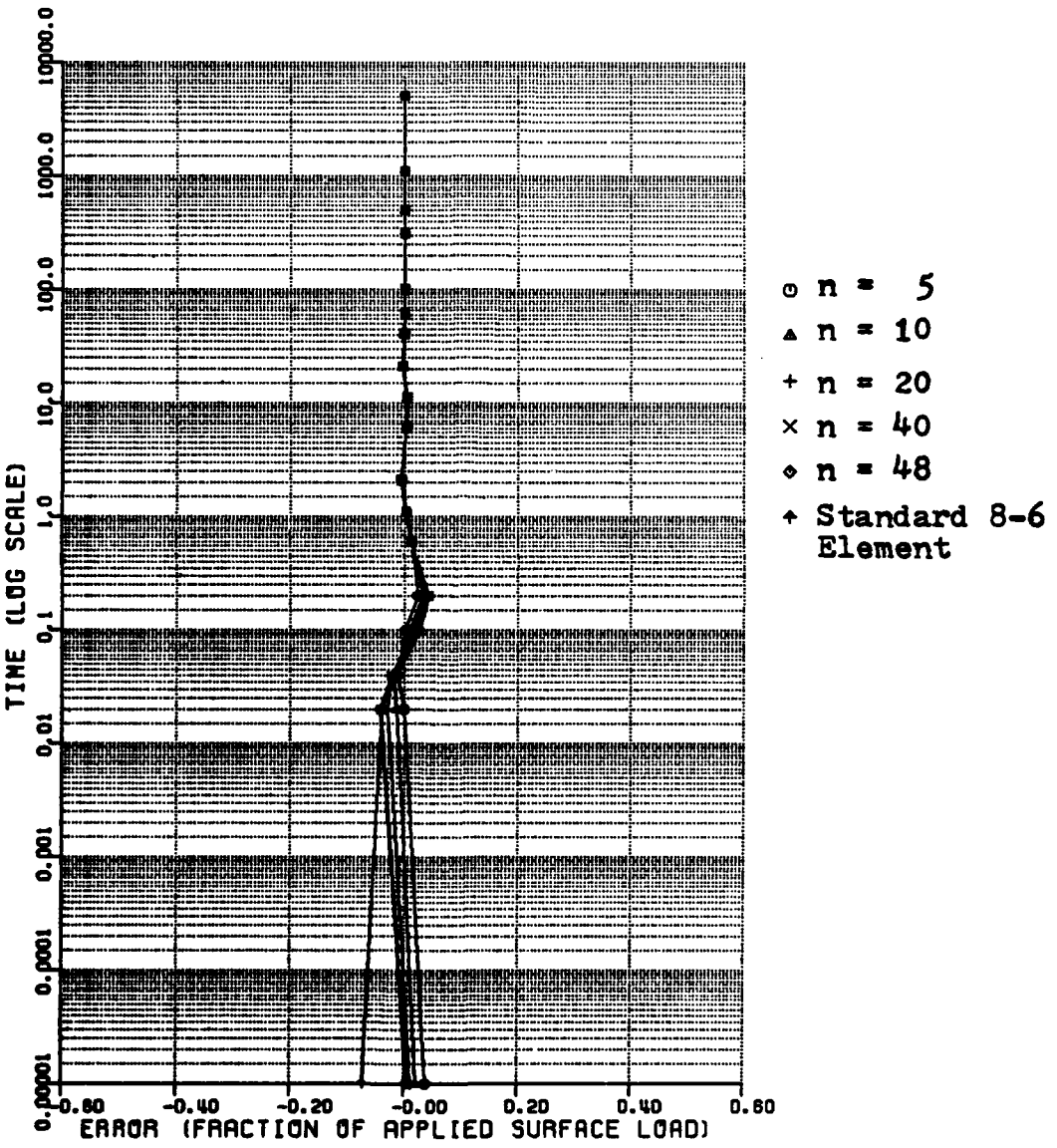

FIGURE 9C DISTRIBUTION OF THE 'RELATIVE' ERROR IN PORE PRESSURE (Special 8-6 Element , Shape Function based on $f(x)=a+bx+cx^n$)

TABLE 3C PORE PRESSURE AT 0.06H BELOW THE SURFACE USING SPECIAL 8-4 ELEMENT (shape function based on $f(x)= a+bx+cx^n$)

τ \ n	5	10	30	40	48	PS84	EXACT
0.0	1.038245	1.022027	1.011728	1.006004	1.005008	0.928240	1.000000
0.000021	0.999230	0.986001	0.971822	0.959741	0.957689	0.961856	1.000000
0.000042	0.987790	0.982048	0.977726	0.978534	0.979522	0.987231	1.000000
0.000105	1.002151	1.009537	1.017353	1.022915	1.023883	1.028603	0.999920
0.000210	1.019010	1.027327	1.032961	1.035481	1.035866	1.037672	0.994710
0.000630	0.905453	0.905477	0.905275	0.905097	0.905060	0.904833	0.892633
0.001154	0.768929	0.768310	0.767870	0.767617	0.767573	0.767321	0.765628
0.002204	0.604722	0.604353	0.604127	0.604007	0.603987	0.603856	0.610575
0.006402	0.390333	0.390289	0.390262	0.390247	0.390245	0.390208	0.386430
0.011650	0.296062	0.296049	0.296042	0.296037	0.296037	0.296013	0.291858
0.022146	0.210361	0.210359	0.210358	0.210358	0.210358	0.210342	0.214009
0.043137	0.153403	0.153402	0.153402	0.153402	0.153402	0.153390	0.154251
0.064128	0.126829	0.126829	0.126828	0.126828	0.126828	0.126819	0.126772
0.106111	0.098956	0.098956	0.098955	0.098955	0.098955	0.098948	0.098701
0.316023	0.052639	0.052639	0.052639	0.052639	0.052639	0.052635	0.052433
0.525936	0.030935	0.030935	0.030935	0.030935	0.030935	0.030933	0.031177
1.155674	0.006326	0.006326	0.006326	0.006326	0.006326	0.006326	0.006592
5.353927	0.000002	0.000002	0.000002	0.000002	0.000002	0.000002	0.0

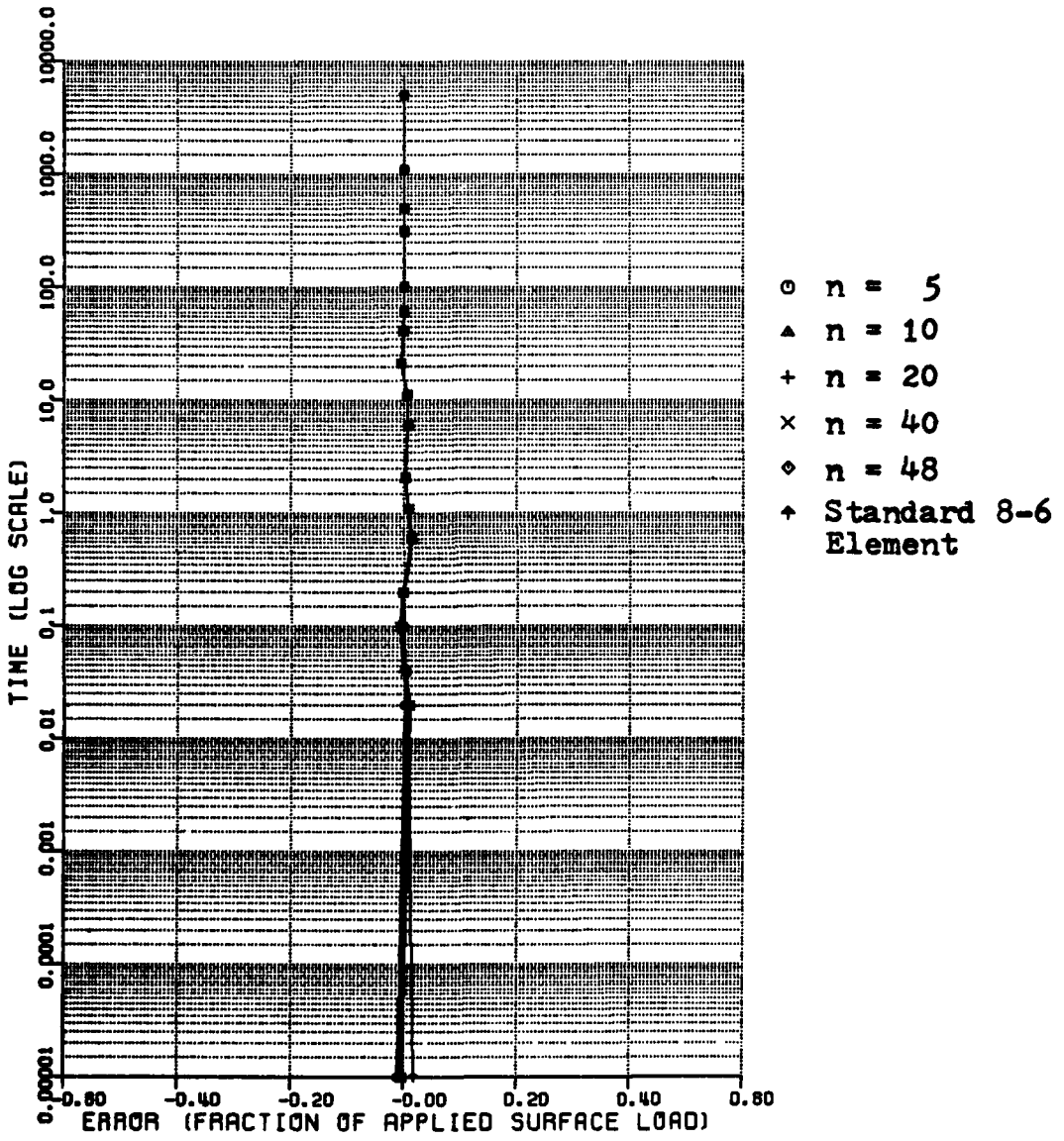

FIGURE 9D DISTRIBUTION OF THE 'RELATIVE' ERROR IN PORE PRESSURE (Special 8-6 Element , Shape Function based on $f(x)=a+bx+cx^n$)

TABLE 3D PORE PRESSURE AT 0.09H BELOW THE SURFACE USING SPECIAL 8-4 ELEMENT (shape function based on $f(x)= a+bx+cx^n$)

τ \ n	5	10	30	40	48	PS84	EXACT
0.0	0.989786	0.994117	0.996868	0.998396	0.998663	1.019164	1.000000
0.000021	1.001270	1.003787	1.006622	1.008934	1.009257	1.006598	1.000000
0.000042	1.003692	1.003699	1.003400	1.002046	1.001565	0.998586	1.000000
0.000105	0.998542	0.995961	0.993606	0.992221	0.992012	0.991172	1.000000
0.000210	0.997317	0.996847	0.996983	0.997436	0.997540	0.998152	0.999971
0.000630	0.997372	0.998653	0.999451	0.999868	0.999938	1.000281	0.984274
0.001154	0.934112	0.934324	0.934415	0.934449	0.934454	0.934463	0.925537
0.002204	0.806147	0.805893	0.805722	0.805626	0.805609	0.805508	0.803293
0.006402	0.558695	0.558652	0.558624	0.558609	0.558607	0.558574	0.551235
0.011650	0.431611	0.431597	0.431587	0.431582	0.431581	0.431559	0.425563
0.022146	0.311415	0.311413	0.311411	0.311410	0.311410	0.311395	0.316197
0.043137	0.228422	0.228421	0.228421	0.228421	0.228421	0.228410	0.229575
0.064128	0.189266	0.189266	0.189266	0.189266	0.189266	0.189257	0.189157
0.106111	0.147959	0.147959	0.147959	0.147959	0.147959	0.147951	0.147578
0.316023	0.078818	0.078818	0.078818	0.078818	0.078818	0.078814	0.078515
0.525936	0.046322	0.046322	0.046322	0.046322	0.046322	0.046320	0.046688
1.155674	0.009473	0.009473	0.009473	0.009473	0.009473	0.009472	0.009871
5.353927	0.000003	0.000003	0.000003	0.000003	0.000003	0.000003	0.0

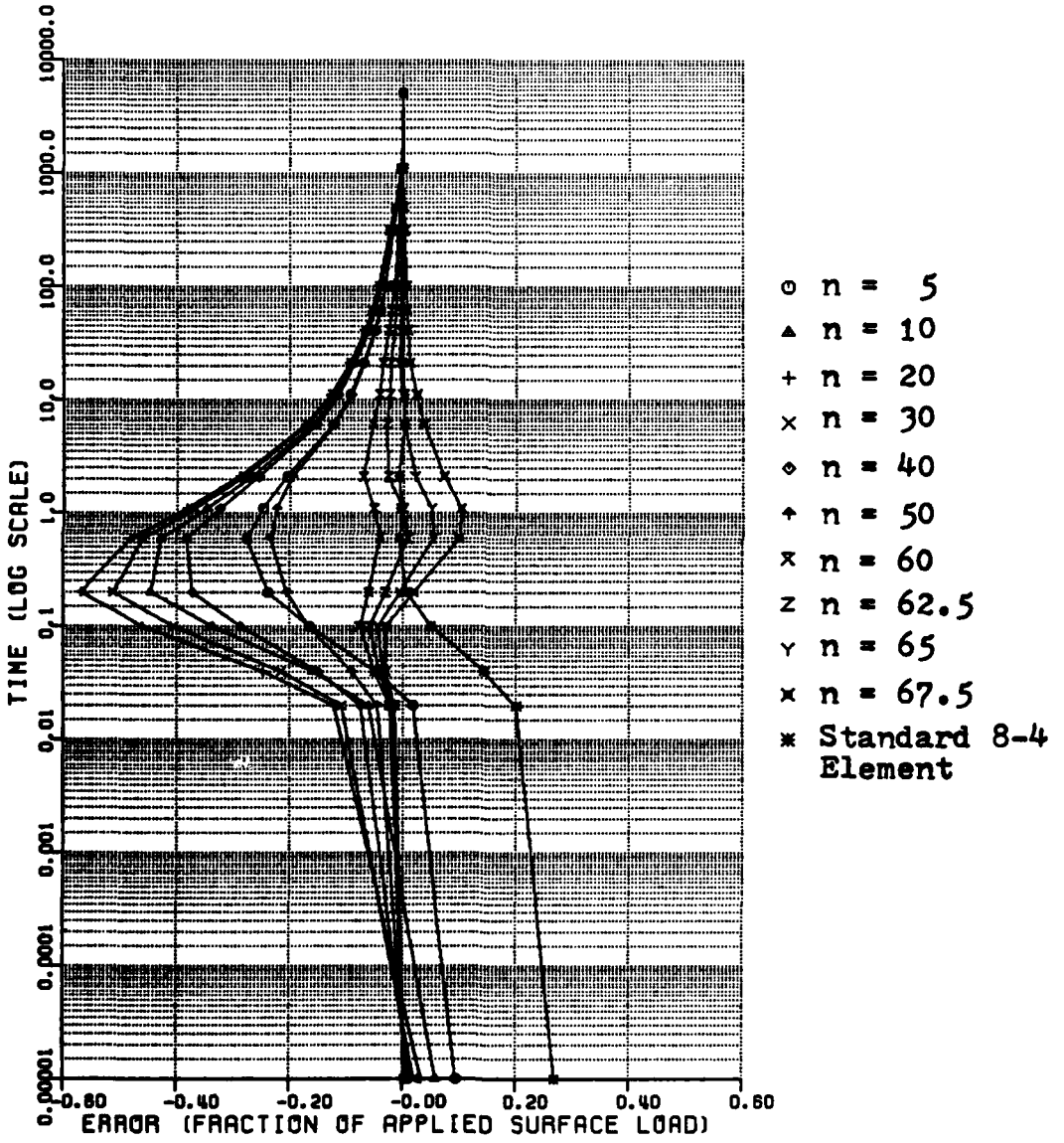

FIGURE 10A DISTRIBUTION OF THE 'RELATIVE' ERROR IN PORE PRESSURE (Special 8-4 Element, Shape Function based on $f(x) = 1-x^n$, 5-point integration)

TABLE 4A PORE PRESSURE AT 0.03H BELOW THE SURFACE USING SPECIAL 8-4 ELEMENT WITH 5-POINT INTEGRATION (shape function based on $f(x)=1-x^n$)

τ \ n	5	10	20	30	40	PS84	EXACT
0.0	1.093962	1.057785	1.032570	1.020553	1.012988	1.267909	1.000000
0.000021	1.018111	0.939977	0.878474	0.891504	0.925370	1.200800	0.999990
0.000042	0.950445	0.839235	0.752152	0.782757	0.848073	1.141744	0.998177
0.000105	0.786365	0.614088	0.491426	0.546508	0.664978	1.001348	0.951382
0.000210	0.598514	0.392097	0.268096	0.325404	0.465278	0.842692	0.836802
0.000630	0.303944	0.155610	0.098615	0.120374	0.197082	0.572994	0.579220
0.001154	0.200307	0.101713	0.066915	0.079392	0.124025	0.443835	0.447879
0.002204	0.128199	0.066812	0.045050	0.052656	0.078720	0.324711	0.333044
0.006402	0.075679	0.040187	0.027274	0.031776	0.047013	0.200795	0.199339
0.011650	0.055474	0.029474	0.020016	0.023306	0.034424	0.150597	0.148478
0.022146	0.038358	0.020411	0.013878	0.016146	0.023800	0.106004	0.107989
0.043137	0.027864	0.014860	0.010113	0.011761	0.017312	0.077033	0.077490
0.064128	0.022985	0.012264	0.008348	0.009708	0.014285	0.063605	0.063587
0.106111	0.017883	0.009544	0.006498	0.007560	0.011114	0.049568	0.049446
0.316023	0.009394	0.004999	0.003400	0.003955	0.005824	0.026345	0.026243
0.525936	0.005404	0.002860	0.001941	0.002259	0.003335	0.015482	0.015604
1.155674	0.001039	0.000541	0.000365	0.000425	0.000632	0.003166	0.003299
5.353927	0.0	0.0	0.0	0.0	0.000002	0.000001	0.0

TABLE 4B PORE PRESSURE AT 0.03H BELOW THE SURFACE SPECIAL 8-4

ELEMENT WITH 5-POINT INTEGRATION (shape function based on $f(x)=1-x^n$)

τ \ n	50	60	62.5	65	67.5	PS84	EXACT
0.0	1.008117	1.005065	1.004499	1.003995	1.003548	1.267909	1.000000
0.000021	0.955571	0.976016	0.979693	0.982882	0.985631	1.200800	0.999990
0.000042	0.907409	0.948727	0.956287	0.962883	0.968605	1.141744	0.998177
0.000105	0.784782	0.875841	0.893234	0.908608	0.922098	1.001348	0.951382
0.000210	0.632305	0.776806	0.806171	0.832607	0.856179	0.842692	0.836802
0.000630	0.345130	0.539599	0.588123	0.634669	0.678542	0.572994	0.579220
0.001154	0.224265	0.396283	0.446831	0.498213	0.549238	0.443835	0.447879
0.002204	0.137805	0.262585	0.306230	0.353959	0.404726	0.324711	0.333044
0.006402	0.079526	0.146111	0.171310	0.200898	0.235193	0.200795	0.199339
0.011650	0.058047	0.106369	0.124800	0.146676	0.172482	0.150597	0.148478
0.022146	0.040002	0.073125	0.085844	0.101064	0.119248	0.106004	0.107989
0.043137	0.029021	0.052834	0.061954	0.072868	0.085925	0.077033	0.077490
0.064128	0.023930	0.043517	0.051013	0.059982	0.070717	0.063605	0.063587
0.106111	0.018610	0.033825	0.039648	0.046618	0.054968	0.049568	0.049446
0.316023	0.009776	0.017852	0.020963	0.024702	0.029202	0.026345	0.026243
0.525936	0.005627	0.010382	0.012238	0.014487	0.017218	0.015482	0.015604
1.155674	0.001083	0.002060	0.002455	0.002945	0.003556	0.003166	0.003299
5.353927	0.000001	0.000001	0.000001	0.000001	0.000001	0.000001	0.0

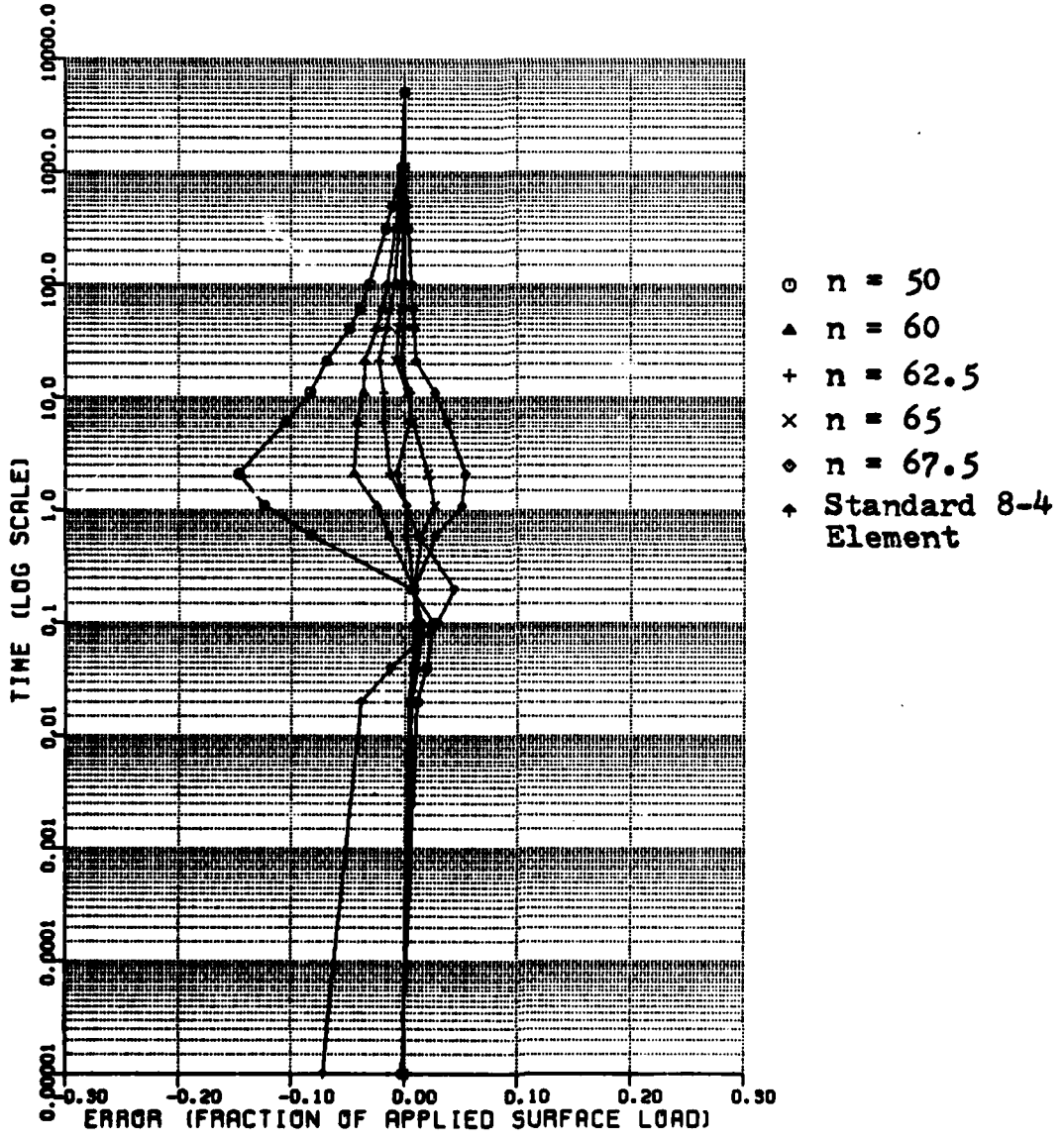

FIGURE 10B DISTRIBUTION OF THE 'RELATIVE' ERROR IN PORE PRESSURE (Special 8-4 Element, Shape Function based on $f(x) = 1-x^n$, 5-point integration)

TABLE 4C PORE PRESSURE AT 0.06H BELOW THE SURFACE SPECIAL 8-4

ELEMENT WITH 5-POINT INTEGRATION (shape function based on $f(x)=1-x^n$)

τ \ n	50	60	62.5	65	67.5	PS84	EXACT
0.0	0.997826	0.998643	0.998795	0.998930	0.999050	0.928240	1.000000
0.000021	1.010637	1.005767	1.004891	1.004130	1.003473	0.961856	1.000000
0.000042	1.019054	1.010612	1.009062	1.007708	1.006532	0.987231	1.000000
0.000105	1.025114	1.014872	1.012857	1.011062	1.009474	1.028603	0.999920
0.000210	1.000578	1.002002	1.002010	1.001946	1.001833	1.037672	0.994710
0.000630	0.811010	0.879184	0.894027	0.907667	0.920047	0.904833	0.892633
0.001154	0.642059	0.741649	0.767351	0.792348	0.816217	0.767321	0.765628
0.002204	0.464511	0.566623	0.598256	0.631252	0.664874	0.603856	0.610575
0.006402	0.282382	0.344879	0.367756	0.394105	0.424006	0.390208	0.386430
0.011650	0.208951	0.256032	0.276350	0.294332	0.318424	0.296013	0.291858
0.022416	0.145643	0.178711	0.191310	0.206310	0.224124	0.210342	0.214009
0.043137	0.106043	0.129756	0.138804	0.149605	0.162490	0.153390	0.154251
0.064128	0.087557	0.107071	0.114520	0.123417	0.134045	0.126819	0.126772
0.106111	0.068178	0.083364	0.089167	0.096105	0.104406	0.098948	0.098701
0.316023	0.035845	0.044050	0.047206	0.050995	0.055551	0.052635	0.052433
0.525936	0.020633	0.025618	0.027559	0.029908	0.032756	0.030933	0.031177
1.155674	0.003973	0.005082	0.005529	0.006080	0.006765	0.006326	0.006592
5.353927	0.000002	0.000002	0.000002	0.000002	0.000002	0.000002	0.0

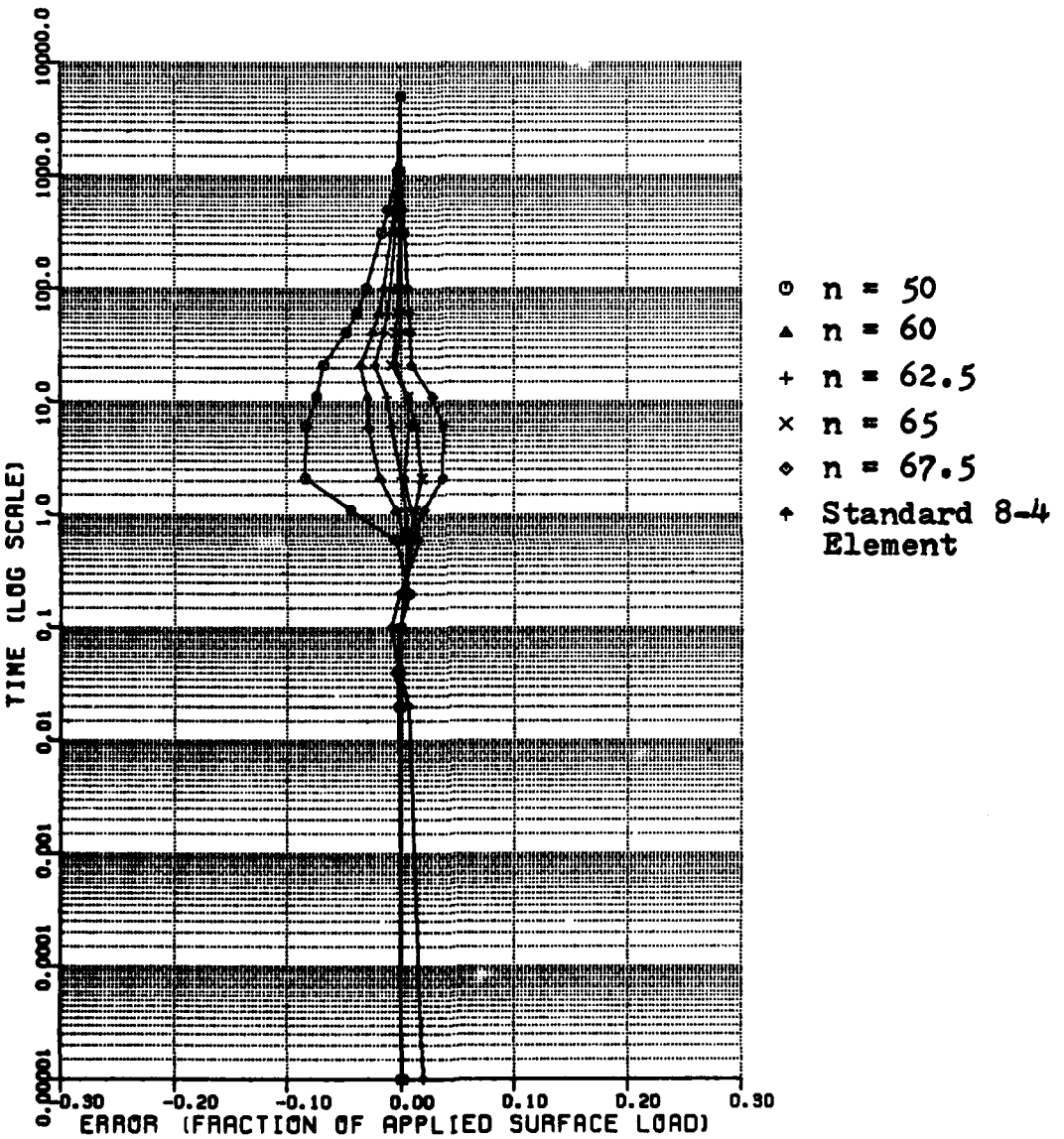

FIGURE 10C DISTRIBUTION OF THE 'RELATIVE' ERROR IN PORE PRESSURE (Special 8-4 Element, Shape Function based on $f(x) = 1-x^n$, 5-point integration)

TABLE 4D PORE PRESSURE AT 0.09H BELOW THE SURFACE SPECIAL 8-4

ELEMENT WITH 5-POINT INTEGRATION (shape function based on $f(x)=1-x^n$)

τ \ n	50	60	62.5	65	67.5	PS84	EXACT
0.0	1.000581	1.000362	1.000322	1.000286	1.000254	1.019164	1.000000
0.000021	0.997466	0.998620	0.998828	0.999008	0.999164	1.006598	1.000000
0.000042	0.996187	0.997861	0.998170	0.998440	0.998675	0.998586	1.000000
0.000105	0.998483	0.998987	0.999105	0.999214	0.999315	0.991172	1.000000
0.000210	1.006289	1.003441	1.002927	1.002481	1.002096	0.998152	0.999971
0.000630	0.979647	0.988652	0.990328	0.991790	0.993058	1.000281	0.984274
0.001154	0.882388	0.920993	0.929963	0.938387	0.946183	0.934463	0.925537
0.002204	0.720058	0.785346	0.803626	0.822006	0.840126	0.805508	0.803293
0.006402	0.468465	0.523309	0.542682	0.564566	0.588891	0.558574	0.551235
0.011650	0.352398	0.396635	0.412879	0.431741	0.453444	0.431559	0.425563
0.022146	0.249027	0.281491	0.293780	0.308293	0.325444	0.311395	0.316197
0.043137	0.182141	0.205539	0.214432	0.225023	0.237621	0.228410	0.229575
0.064128	0.150644	0.169965	0.177319	0.186091	0.196548	0.189257	0.189157
0.106111	0.117485	0.132584	0.138344	0.145225	0.153446	0.147951	0.147578
0.316023	0.061835	0.070153	0.073348	0.077181	0.081785	0.078814	0.078515
0.525936	0.035595	0.040801	0.042824	0.045268	0.048227	0.046320	0.046688
1.155674	0.006854	0.008095	0.008592	0.009203	0.009960	0.009472	0.009871
5.353927	0.000004	0.000004	0.000004	0.000003	0.000003	0.000003	0.0